SEMI-ANNUAL TECHNICAL REPORT

1 JANUARY 1960 - 30 JUNE 1960

CONTRACT NO. AF49 (638) -658

PROJECT NO. 4766, TASK NO. 11

ARPA ORDER NO. 6-58

RESEARCH ON PLASMA ACCELERATION BY ELECTRIC FIELD GRADIENT

JUNE 1960

PREPARED FOR...

UNITED STATES AIR FORCE

OFFICE OF SCIENTIFIC RESEARCH

WASHINGTON, D.C.

PREPARED BY...

ASTRO-ELECTRONICS DIVISION AND RCA LABORATORIES

RADIO CORPORATION OF AMERICA

PRINCETON, NEW JERSEY

CLEARINGHOUSE FOR FEDERAL SCIENTIFIC AND TECHNICAL INFORMATION, CFSTI
INPUT SECTION 410.11

LIMITATIONS IN REPRODUCTION QUALITY OF TECHNICAL ABSTRACT BULLETIN DOCUMENTS, DEFENSE DOCUMENTATION CENTER (DDC)

AD 613307

☐ 1. AVAILABLE ONLY FOR REFERENCE USE AT DDC FIELD SERVICES. COPY IS NOT AVAILABLE FOR PUBLIC SALE.

☒ 2. AVAILABLE COPY WILL NOT PERMIT FULLY LEGIBLE REPRODUCTION. REPRODUCTION WILL BE MADE IF REQUESTED BY USERS OF DDC.

☒ A. COPY IS AVAILABLE FOR PUBLIC SALE.

☐ B. COPY IS NOT AVAILABLE FOR PUBLIC SALE.

☐ 3. LIMITED NUMBER OF COPIES CONTAINING COLOR OTHER THAN BLACK AND WHITE ARE AVAILABLE UNTIL STOCK IS EXHAUSTED. REPRODUCTIONS WILL BE MADE IN BLACK AND WHITE ONLY.

TSL-121-2/64

DATE PROCESSED: 13 Apr 65

PROCESSOR: EMJ

SEMI-ANNUAL TECHNICAL REPORT

1 JANUARY 1960--30 JUNE 1960

CONTRACT NO. AF49 (638) -658

PROJECT NO. 4766, TASK NO.11

ARPA ORDER NO. 6-58

RESEARCH ON PLASMA ACCELERATION BY ELECTRIC FIELD GRADIENT

JUNE 1960

PREPARED FOR...

UNITED STATES AIR FORCE

OFFICE OF SCIENTIFIC RESEARCH

WASHINGTON, D.C.

PREPARED BY...

ASTRO-ELECTRONICS DIVISION AND RCA LABORATORIES

RADIO CORPORATION OF AMERICA

PRINCETON, NEW JERSEY

TABLE OF CONTENTS

TABLE OF CONTENTS (cont.)

LIST OF ILLUSTRATIONS

BLANK PAGE

PURPOSE OF CONTRACT

The immediate objective of the research described herein is to demonstrate experimentally the acceleration of a plasma by an alternating electric field with an amplitude gradient, and to develop an understanding of the underlying principles of such means of acceleration, especially as may be applicable to electronic rocket propulsion. The contract began on June 15, 1959, and extends to June 15, 1960. This report covers work performed from December 15, 1959 to June 15, 1960; the results of the first six months' effort were reported previously.[1]

The Astro-Electronics Division of RCA has responsibility for the contract research, which is under the general supervision of E. C. Hutter, Manager, Physical Research. The Astro-Electronics Division of RCA is being assisted in the project by members of the Microwave and Plasma Group of RCA Laboratories, under the leadership of L. S. Nergaard and M. Glicksman. The experimental work itself is being carried out at the David Sarnoff Research Center, RCA Laboratories. The following personnel worked on the project during the period covered in this report.

G. D. Gordon	Astro-Electronics Division
H. W. Lorber	RCA Laboratories
L. S. Napoli	RCA Laboratories
T. T. Reboul	Astro-Electronics Division
G. A. Swartz	RCA Laboratories

Consultation has been furnished by K. G. Hernqvist of RCA Laboratories.

ABSTRACT

Theoretical studies[1] of plasma acceleration by an rf field gradient indicated that a plasma will be accelerated toward the low-field region if the applied frequency is greater than the critical frequency of the plasma, and toward the high-field region if the frequency is less than the critical frequency. Calculations for the acceleration of plasma spheres and ellipsoids of arbitrary orientation with respect to the rf field have been completed. Experiments with plasmas of various densities have demonstrated both the acceleration and deceleration of the plasmas as predicted by theory. Mercury plasma has been accelerated with a 140-Mc rf field gradient to a velocity of 25×10^5 cm/sec, equivalent to a specific impulse of 2500 seconds.

I. INTRODUCTION

The use of charged particles for rocket propulsion appears very attractive and is under investigation in a number of laboratories at the present time.[2] The primary advantages of such a system over the present chemical or mechanical system are the high specific impulse generated and the relatively small mass of working fluid required. The investigations on charged particles cover work on both ion and plasma acceleration. Ions provide thrust when accelerated by electrostatic fields. Several mechanisms exist for obtaining thrust from plasmas (a neutral mixture of ions and electrons). The plasma may be heated electrically[3], and the thrust provided by ejecting the energetic particles from the rocket. The plasma may be accelerated also by means of crossed electric and magnetic fields[4] or by rapidly changing magnetic fields.[5] In addition, previous work at RCA Laboratories and at other laboratories have indicated the possibility of both containment[6-12] and acceleration[13,14] of a plasma by a non-uniform rf electric field. This latter method is especially attractive because it eliminates the need for heavy magnetic field structures in the plasma case and eliminates the space-charge problems associated with the diode-type electrostatic ion accelerators.

The work reported herein has been concerned with the demonstration of the acceleration of plasma by means of an rf field gradient and deals primarily with work of the last six months. During the first six months of this study the major experimental work included setting up the proper equipment and performing preliminary experiments. During that period, a theory based on a two-particle plasma model that predicted the force exerted on an infinite-slab plasma by an rf field gradient was developed. During the last six months, experimental work has been concerned primarily with measuring plasma densities and with demon-

strating plasma acceleration and deceleration. The theoretical work has been expanded to permit calculations of forces on plasmas with more realistic shapes, to explain some of the experimental data obtained, and to suggest future experimental work.

II. THEORY

A. INTRODUCTION

A theory of plasma acceleration by rf field gradient based on energy considerations has been developed. In its simplest form, the theory yields the same acceleration for a plasma slab as the previous theory of T. V. Johnston.[1] The theory is based on the macroscopic plasma properties, rather than the motion of individual particles considered in Johnston's theory. Fewer and more straightforward assumptions are made, and the results have been shown to be valid for a wider range of conditions. The theory can easily be extended to other geometries; the acceleration of plasma ellipsoids has been calculated, and the results are given. The theory can also be extended to non-uniform plasmas, and the possibilities and advantages of such extensions are discussed in section C. The magnitude of the effect of certain assumptions on the theory has also been considered. The effect of a dc bias in addition to the rf voltage on the electrodes has been considered theoretically and the results are presented in Appendix A.

B. ACCELERATION OF A PLASMA SLAB

The velocities attainable with rf field gradient acceleration can be calculated on the basis of energy considerations as follows: The energy density of an rf electric field of amplitude E is

$$\frac{1}{4}\epsilon_o E^2 \qquad (1)$$

where ϵ_o is the permittivity of free space. When a plasma in the form of a thin slab with boundaries perpendicular to the electric field is introduced into the field, so that the displacement D remains constant, the electric energy density inside the plasma is

$$Re\left[\frac{1}{4}\ \frac{D^2}{K\epsilon_o}\right] = Re\left[\frac{1}{4}\ \frac{\epsilon_o E^2}{K}\ \right] \tag{2}$$

where E, as defined above, is the field present before the plasma was introduced. The magnetic energy need not be considered if there is no applied magnetic field and if the rf field can be considered a quasi-static electric field. The dielectric constant K of the plasma is[15]

$$K = \frac{\omega_p^2 - \omega^2 + i\,\omega\,\nu}{-\omega^2 + i\,\omega\,\nu} \tag{3}$$

where ω is the frequency of the rf field, ν the electron collision frequency, and ω_p the plasma frequency. The plasma frequency is defined by

$$\omega_p^2 = \frac{ne^2}{\epsilon_o}\left(\frac{1}{m} + \frac{1}{M}\right) \approx \frac{ne^2}{m\epsilon_o} \tag{4}$$

The potential energy U of the plasma is equal to the difference between the electric energy density inside the plasma and the energy density present without the plasma:

$$U = Re\left[\frac{1}{4}\ \frac{\epsilon_o E^2}{K} - \frac{1}{4}\ \epsilon_o E^2\right] = \frac{1}{4}\ \epsilon_o E^2\ \frac{\omega_p^2(\omega^2-\omega_p^2)}{(\omega^2-\omega_p^2)^2+(\omega\nu)^2} \tag{5}$$

It is assumed in what follows that the plasma density is constant, that the shape of the plasma slab is not determined by the field, and that the motion of the particles in the plasma is small during each period of the rf field. If the plasma moves to a zero field region and if the change in electric energy density is transformed into translational energy, then

$$U = \frac{1}{2}\ \rho\ v_f^2 - \frac{1}{2}\ \rho\ v_i^2 \tag{6}$$

where ρ is the mass density of the plasma, v_f is the final velocity and v_i is the initial velocity. Thus the plasma attains a final velocity at zero field of

$$v_f = \left\{ v_i^2 + \frac{e^2E^2}{2mM} \left(\frac{\omega^2 - \omega_p^2}{(\omega^2-\omega_p^2)^2 + (\omega\nu)^2} \right) \right\}^{1/2} \tag{7}$$

As defined above, E is the applied field and therefore is independent of changes in the actual electric field due to the plasma. It should be noted that this final velocity will be greater than the initial velocity only if the applied frequency is greater than the plasma frequency.

For comparison with theories of plasma confinement, the mechanical force exerted on the plasma can be obtained by calculating the variation of the potential energy U with respect to a small displacement. The force (f) on the plasma is

$$f = -\nabla U = \frac{ne^2}{4m} \nabla E^2 \frac{\omega_p^2 - \omega^2}{(\omega_p^2-\omega^2)^2 + (\omega\nu)^2} \tag{8}$$

The mechanism of the energy transfer can be understood physically by considering the polarization of the plasma in the electric field gradient. For high density plasmas $(\omega_p > \omega)$, the polarization P is in the same direction as the applied field, and therefore a force $P \cdot \nabla E$ exists in the direction of the field gradient. For low density plasmas $(\omega_p < \omega)$ the polarization is in the opposite direction and the force is reversed.

C. EXTENSIONS OF THE THEORY

One of the principal advantages of the theory based on energy considerations is the possibility for extensions to more general cases. The acceleration of a plasma of any geometry can be calculated by substituting a dielectric for the plasma and calculating the static electric field configuration. An extension of

the theory to plasma ellipsoids is given in Appendix B. Special cases can then be computed, including the acceleration of a slab, a sphere, and a flat disk by varying the ratio of major to minor axis. These calculations show that the major effect of geometry changes is a change in resonant frequency. The resonant frequency for all other shapes is always less than that for a slab perpendicular to the electric field. For a long needle of plasma, parallel to the rf field, the resonant frequency decreases rapidly as the length-to-width ratio increases.

The assumption that the plasma density is uniform is a difficult condition to realize in practice. In the present experiment the density varies by a factor of 100 in the accelerating region. In the theory based on energy considerations, the problem is equivalent to an electric potential problem with variable dielectric constant. While such problems are difficult to handle, they can be solved in principle. The problem of concentric spherical shells of different densities has been considered. One of the principal results is that resonance no longer occurs at a single frequency, but occurs at several frequencies.

D. ASSUMPTIONS IN THE THEORY

The major theoretical assumption is that the energy within the plasma in the rf field will be converted into translational energy. For the neutral and ion densities reported in the following experiment, the mean free path is too long for scattering or turbulence to occur. Hence the field energy is not lost as heat. Another possibility is that the field energy is converted to an alternating motion of the electrons rather than an overall drift. The fraction of the field energy converted to drift depends on how the rf field varies from the maximum field region to the minimum field region. If the field drops abruptly, the energy will not be converted into translational energy. In the latter case the plasma oscillations will continue in the zero field region and the energy will eventually be converted into thermal energy. The critical field gradient is not determined by the present theory, but in Appendix C it is shown that the limit is approximate.

$$\frac{dE}{dZ} \gtrsim \frac{m}{e} \omega_p^2 \tag{9}$$

To accelerate a plasma which starts in a zero field region, the field gradient should be greater than the critical value until the point of maximum field is reached, so that the plasma is not decelerated by the rf field; then the rf field should decrease at such a rate that the field gradient is less than the critical value, so that the plasma can be effectively accelerated. In Appendix C the effects on plasma acceleration as the field gradient approaches the critical value are investigated.

E. CONCLUSIONS

Plasma velocities that can be attained by rf acceleration are given by Equation 7. The final theoretical velocity for a mercury plasma can be plotted as a function of the applied frequency, the result being the resonance curve shown in Figure 1. The effect of the initial velocity is to increase the final velocity, and for simplicity an initial velocity of zero was chosen. The effect of the electron collision frequency is a decrease in the maximum velocities near resonance, but little change at frequencies far from resonance, as demonstrated by the two curves in the Figure. Calculated electron collision frequencies for the experimental plasmas are much lower than the values chosen for illustration, but it is expected that density variations not considered in the theory will reduce the maximum resonance and effectively increase the total damping. In terms of the present theory the maximum final velocity occurs at $\omega^2 = \omega_p^2 + \omega_p \nu$ and has the value

$$v_{f(max)} = \left\{ v_i^2 + \frac{e^2 E^2}{2mM(2\omega_p \nu + \nu^2)} \right\}^{1/2} \tag{10}$$

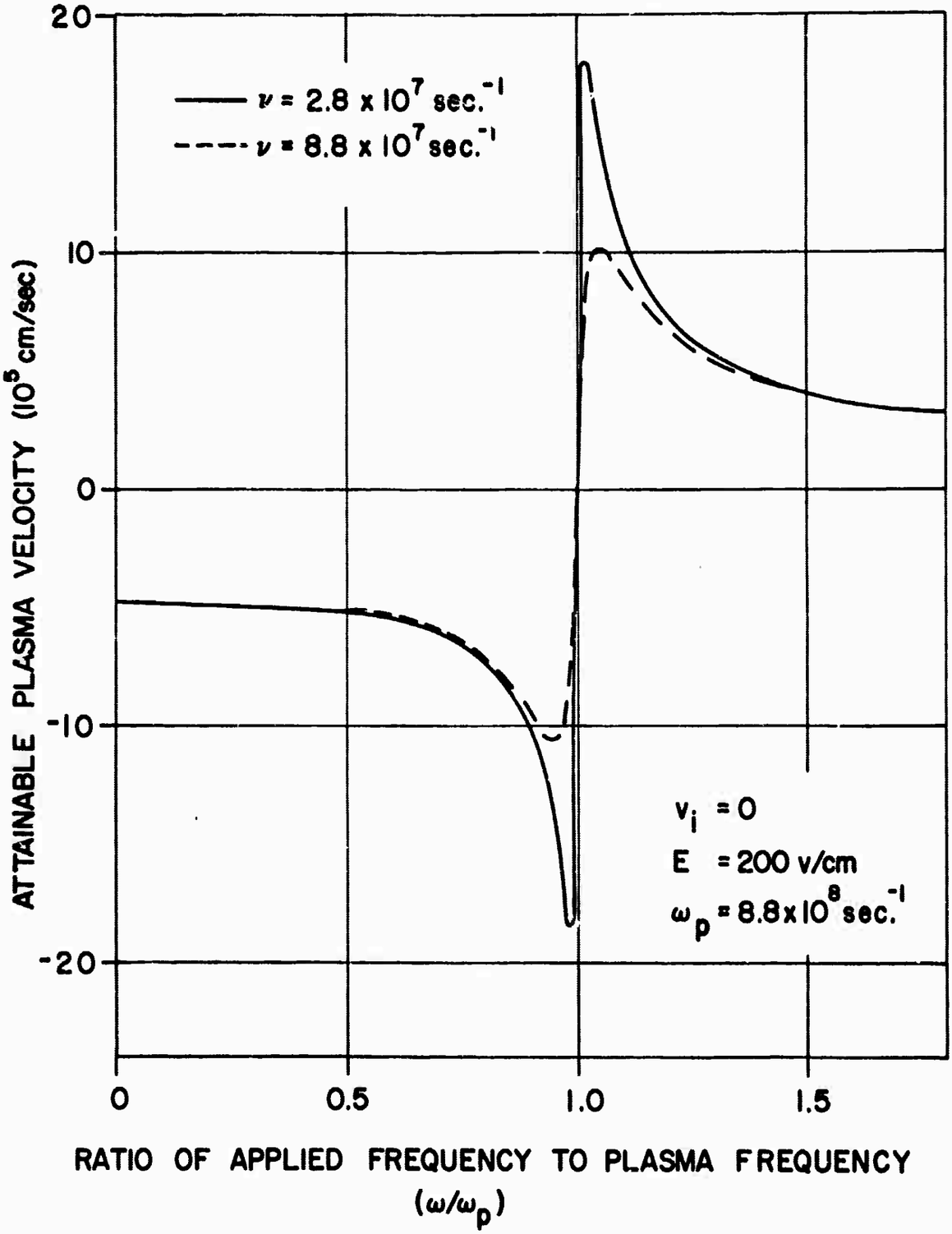

Figure 1. Theoretical Final Velocities of Plasma as a Function of Applied Frequency

At this point the acceleration is toward the field minimum, and this is the optimum condition for practical applications.

For Figure 1 the magnitude of the applied rf field was chosen as 200 v/cm, a value easily attainable. The dependence of final velocity on the magnitude of the applied rf field is illustrated in Figure 2. If the initial velocity is zero the final velocity is proportional to the electric field. When the initial velocity is appreciable, the curve is a hyperbola, the slope of the asymptote being a function of ω/ω_c as shown in the Figure. In Section V the theoretical curves will be compared with the results obtained experimentally.

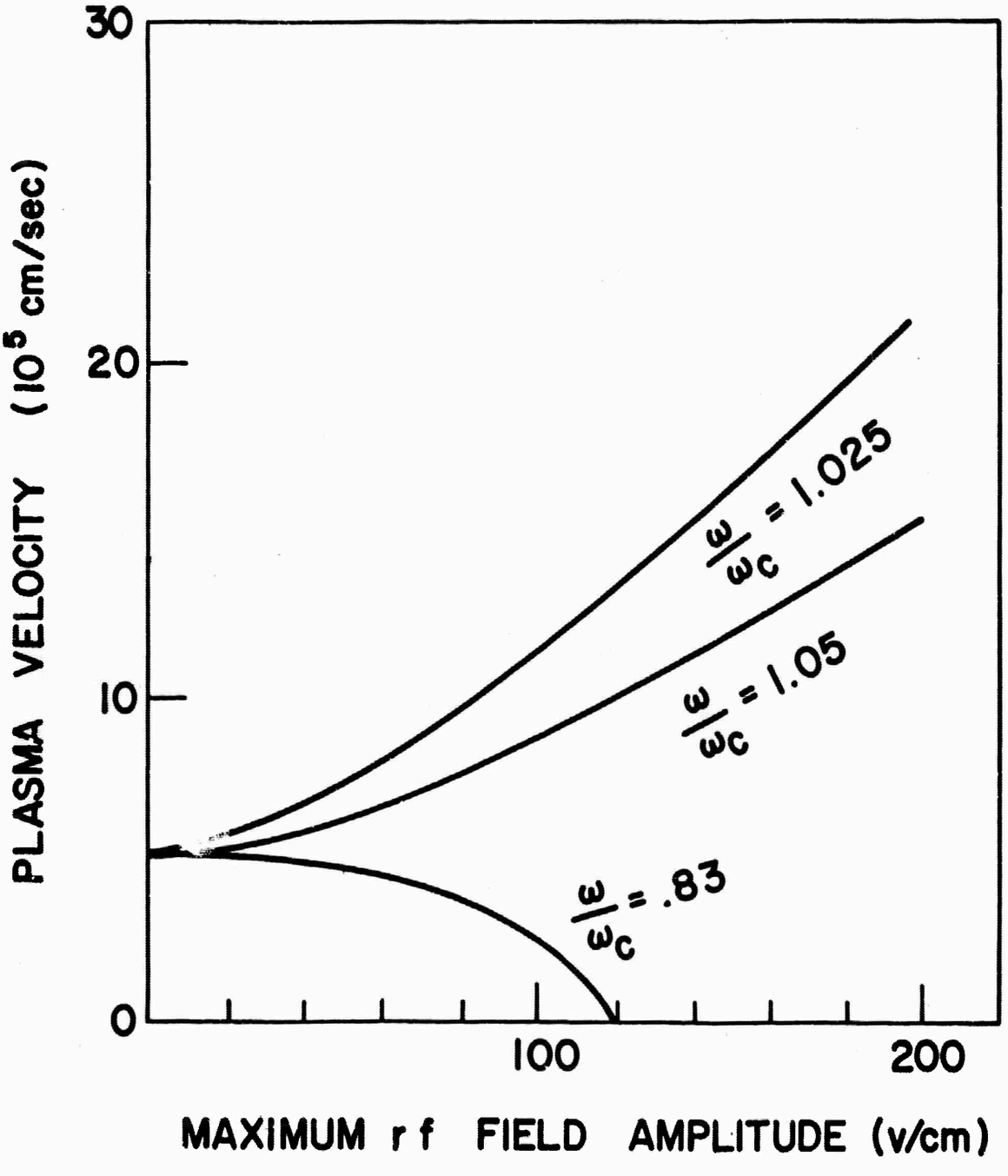

Figure 2. Theoretical Final Velocities of Plasma as a Function of rf Field

III. APPARATUS

A. INTRODUCTION

The apparatus described in this report was built to show experimentally that a non-uniform rf field can exert a force on a plasma. The apparatus as shown in Figure 3 consists of a plasma source in an evacuated envelope fitted with plasma detectors and an rf electrode system.

B. PLASMA SOURCE

The plasma source supplies pulses of mercury plasma. The pulse length is approximately 100 microseconds. The igniter type source, which was developed during the first six months of this study, consists of a silicon carbide igniter dipped into a pool of mercury. The igniter is energized by discharging 6 joules from an energy storage capacitor. The discharge is controlled by a thyratron switch that closes at a specific voltage.

The density of the plasma pulse in the rf interaction region is varied by adjusting the size of the source orifice. A source aperture of 2.5 mm diameter provides a maximum density of about 10^{10} ions per cubic centimeter at an axial distance of 1 centimeter from the source.

A source that incorporates a plasma shutter was constructed to decrease the length of the plasma pulse. Such an effect should provide means for increasing the accuracy and reliability of time-of-flight measurements. A diagram of the shutter is given in Figure 4. This shutter is being tested at the present time.

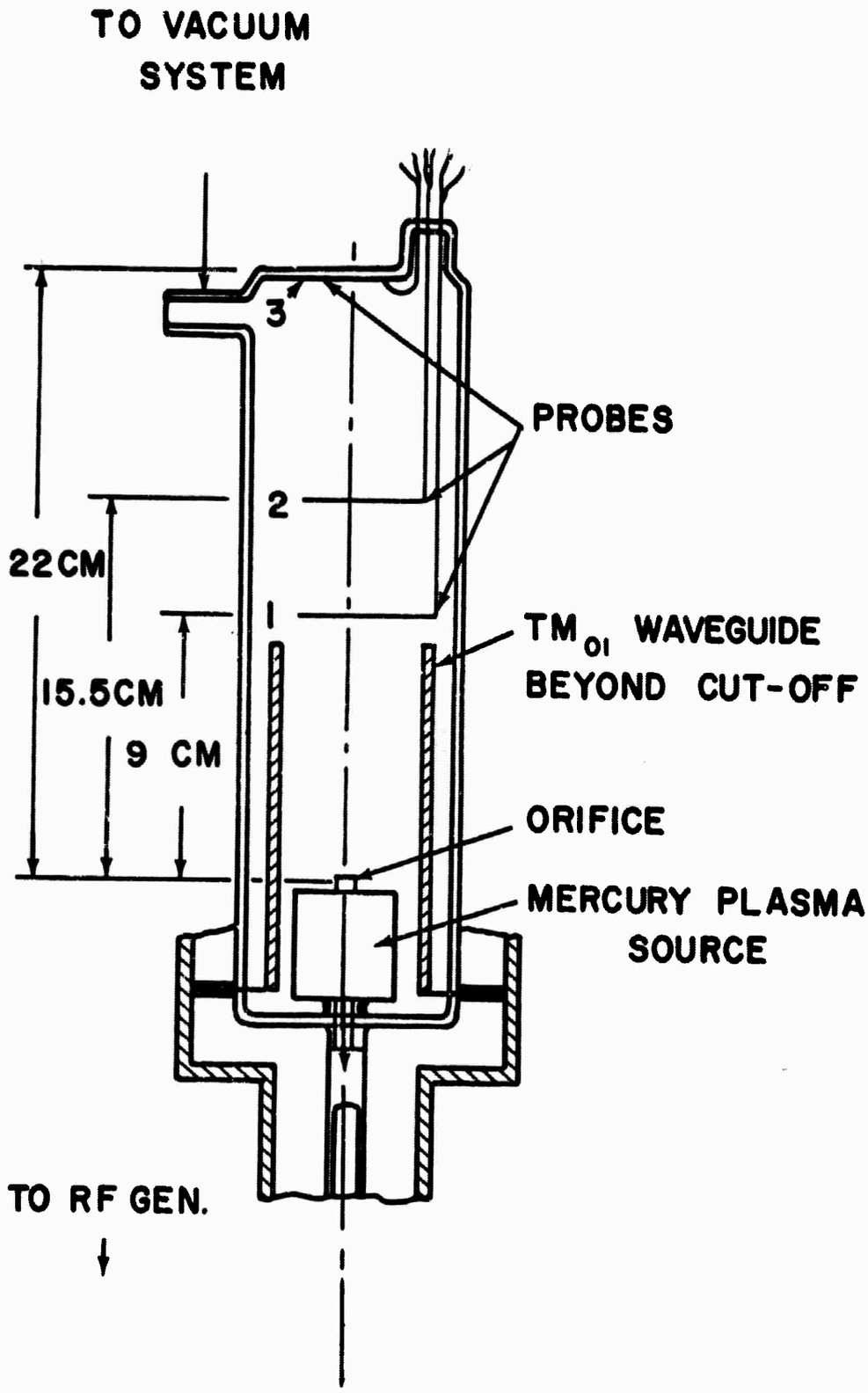

Figure 3. Experimental Apparatus

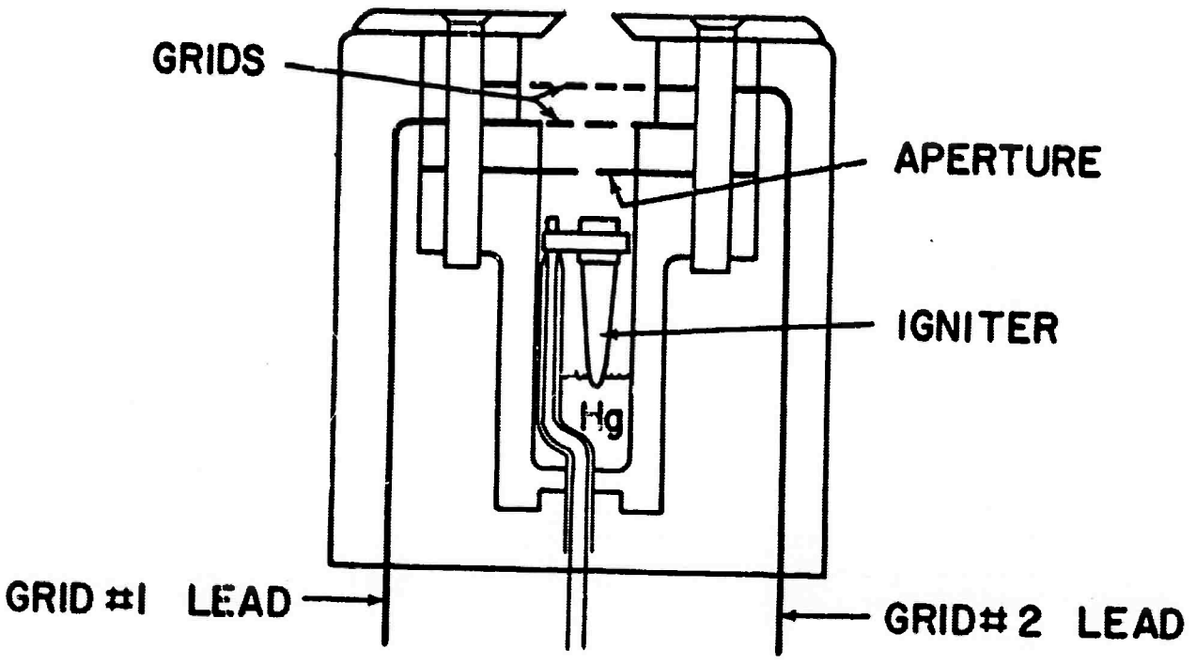

Figure 4. Electronic Shutter for Plasma Source

C. THE RF SYSTEM

The rf acceleration system is shown in Figure 3. It consists of a plasma source on the end of the inner conductor of the rf feed and looks into a cut-off waveguide. The electrode structure was designed to produce a field maximum very near the orifice.

A measurement of electric field along the axis both outside the source and inside the orifice was made by the use of a resistance-board analog. The axial electric field distribution as determined by this method is given in Figure 5. The axial field decreases to 1/10 maximum in less than 3 centimeters.

The magnitude of the electric field E off the axis is shown in Figure 6. Because the energy of the plasma depends upon the square of the electric field, contours of E^2, rather than E, near the orifice have been plotted.

Details of the rf system are contained in a previous report. Both a 140-Mc and a 300-Mc generator have been used for the acceleration experiments.

D. EVACUATED ENVELOPE AND VACUUM SYSTEM

The evacuated tube envelope and vacuum system were described in detail in a previous report.[1] Experiments have been conducted with the evacuated envelope continually pumped. The upper half of the evacuated envelope is covered with dry ice to reduce the ambient pressure caused by the mercury from the source. This procedure was followed in all experiments to prevent an rf discharge in the enclosure during measurements. Pressure in the system is measured by a Pirani gauge

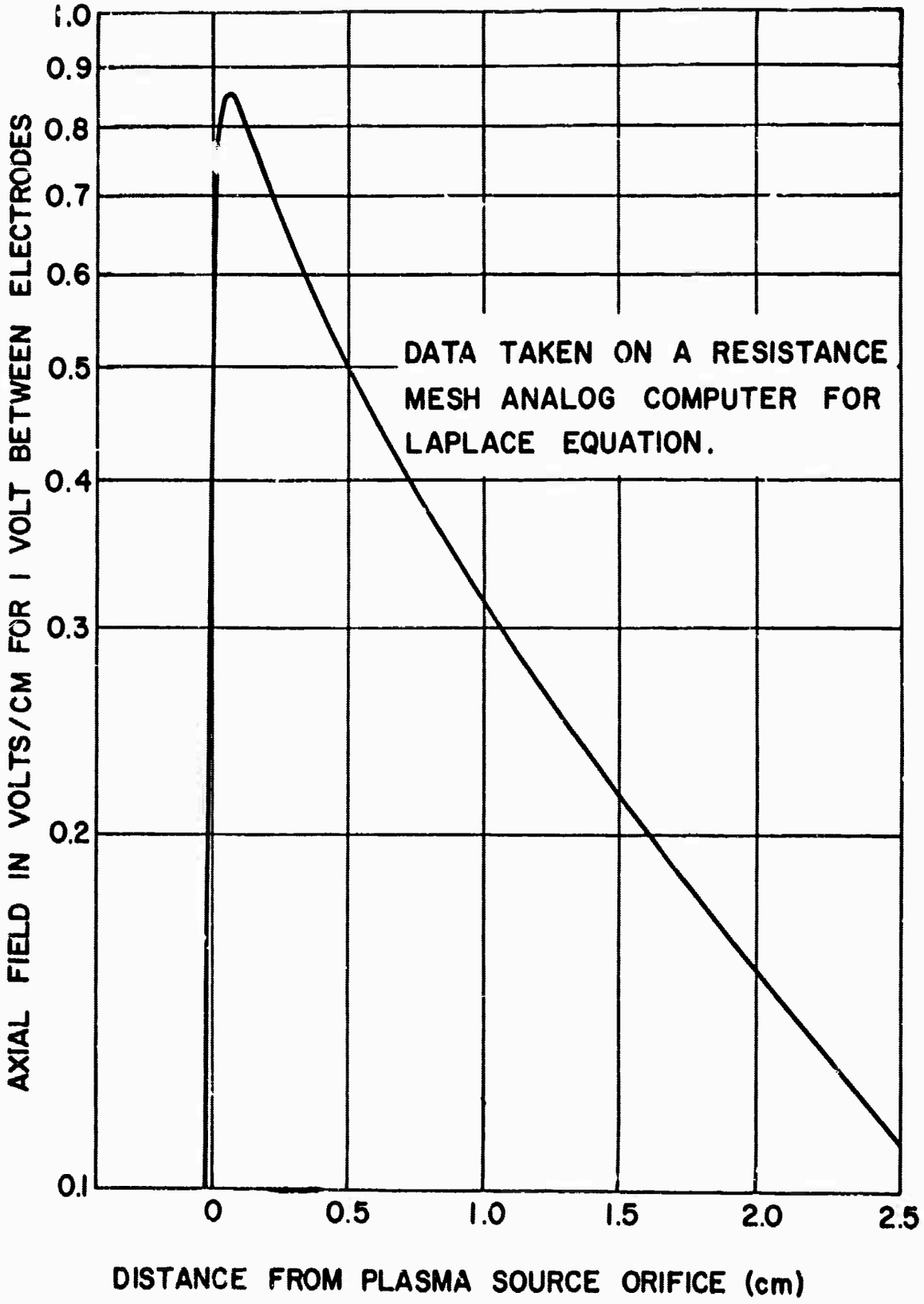

Figure 5. Magnitude of RF Electric Field On Axis

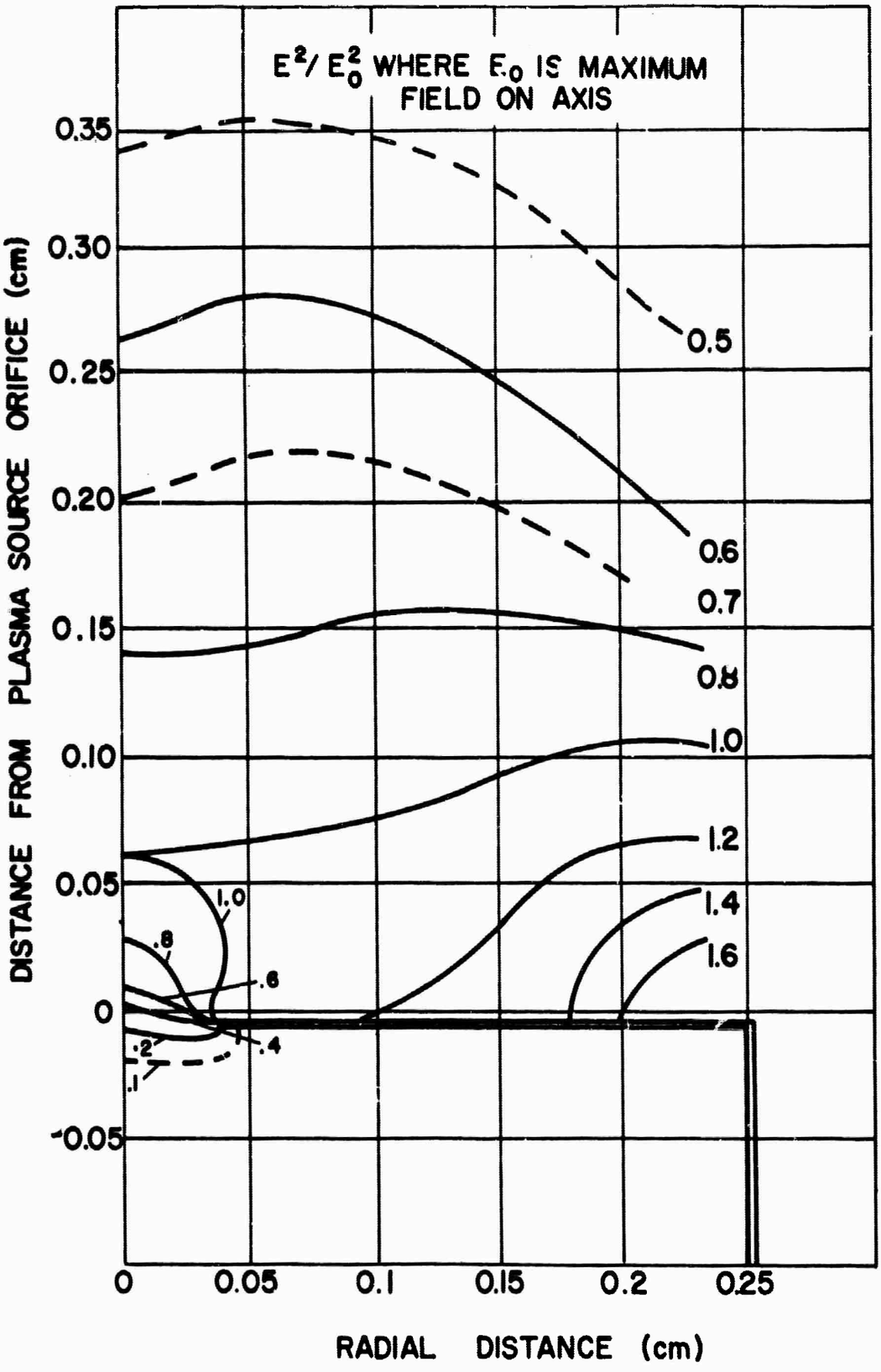

Figure 6. Magnitude of RF Electric Field Off Axis

and an ionization gauge. The vacuum system is capable of pumping down to a pressure of 10^{-6} mm Hg with the system unbaked.

E. DIAGNOSTICS

The plasma source described in this report was designed to provide pulses of plasma less than a millisecond in duration. The average and final velocities of these pulses have been determined by measuring their transit times from the source to a probe and between two probes, respectively. Both single and double wire probes have been used. Each probe is mounted normal to the axis of the envelope as shown in Figure 3.

IV. EXPERIMENTAL RESULTS

A. PLASMA CHARACTERISTICS

Several characteristics of the plasma pulse were investigated under conditions of zero rf field. Measurement of the plasma diffusion velocity was made previously. In the last six months, density and electron temperature of the plasma were determined in the region near the source orifice. These parameters were determined by single-probe measurements. Various potentials with respect to ground were applied to the probe and the peak of the current was recorded as the plasma passed by the probe. Plasma density and electron temperature were determined by an analysis of the resulting current voltage curve. A typical curve is shown in Figure 7.

Electron temperature is determined from the slope, and the charge density from the value of the current at which the curve departs from an exponential dependence[16] on voltage. Measured density contours near the source with an 0.8-mm orifice are shown in Figure 8. In Figure 9 are plotted curves of density vs. distance along the axis of the tube for .8-mm and 2.5-mm source apertures.

The electron temperature of the plasma was about 20,000°K for a 300-volt discharge in the igniter source. For a discharge voltage of 400 volts, the electron temperature was 29,000°K, but the plasma density remained substantially the same.

The probe system described in Section III was used to measure the drift velocity of the plasma. Figure 10 shows the ion and electron currents to the first probe as a function of time. The electrons arrive at the probes before the ions, indicating ambipolar diffusion. Plasma velocity was determined by measuring the time of

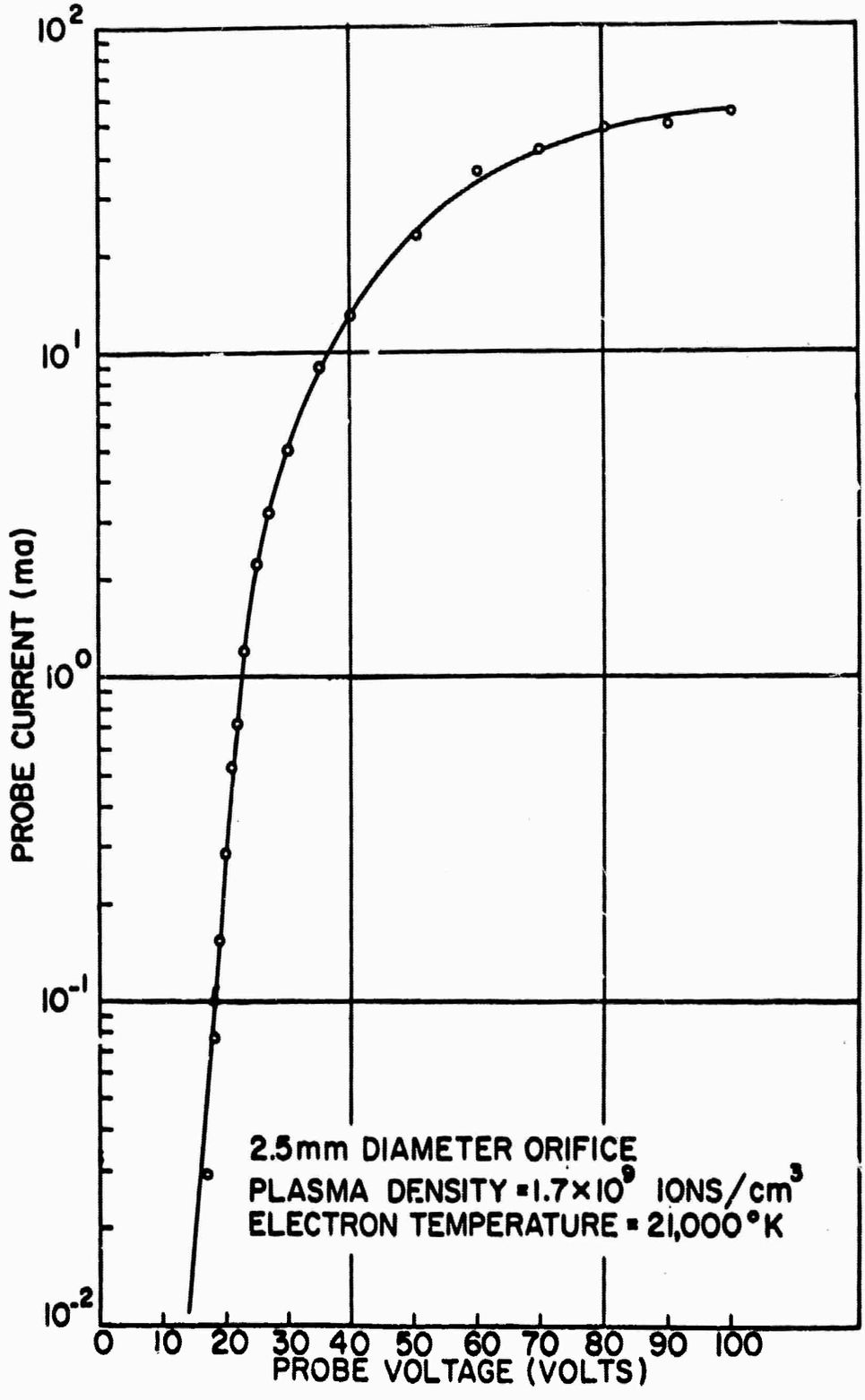

Figure 7. Single Probe Characteristic I-V Curve

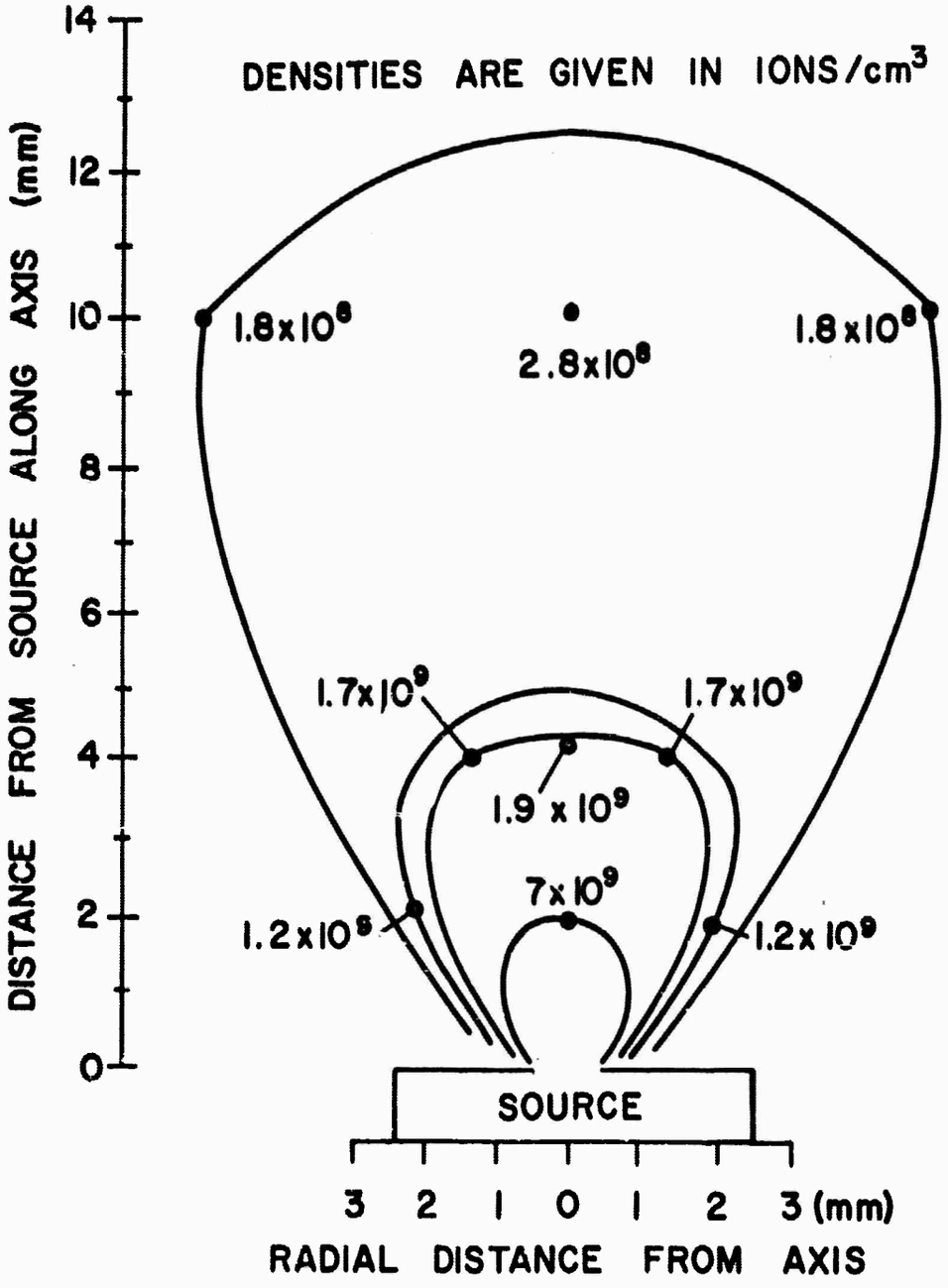

Figure 8. Plasma Density Contour near 0.8 mm Orifice

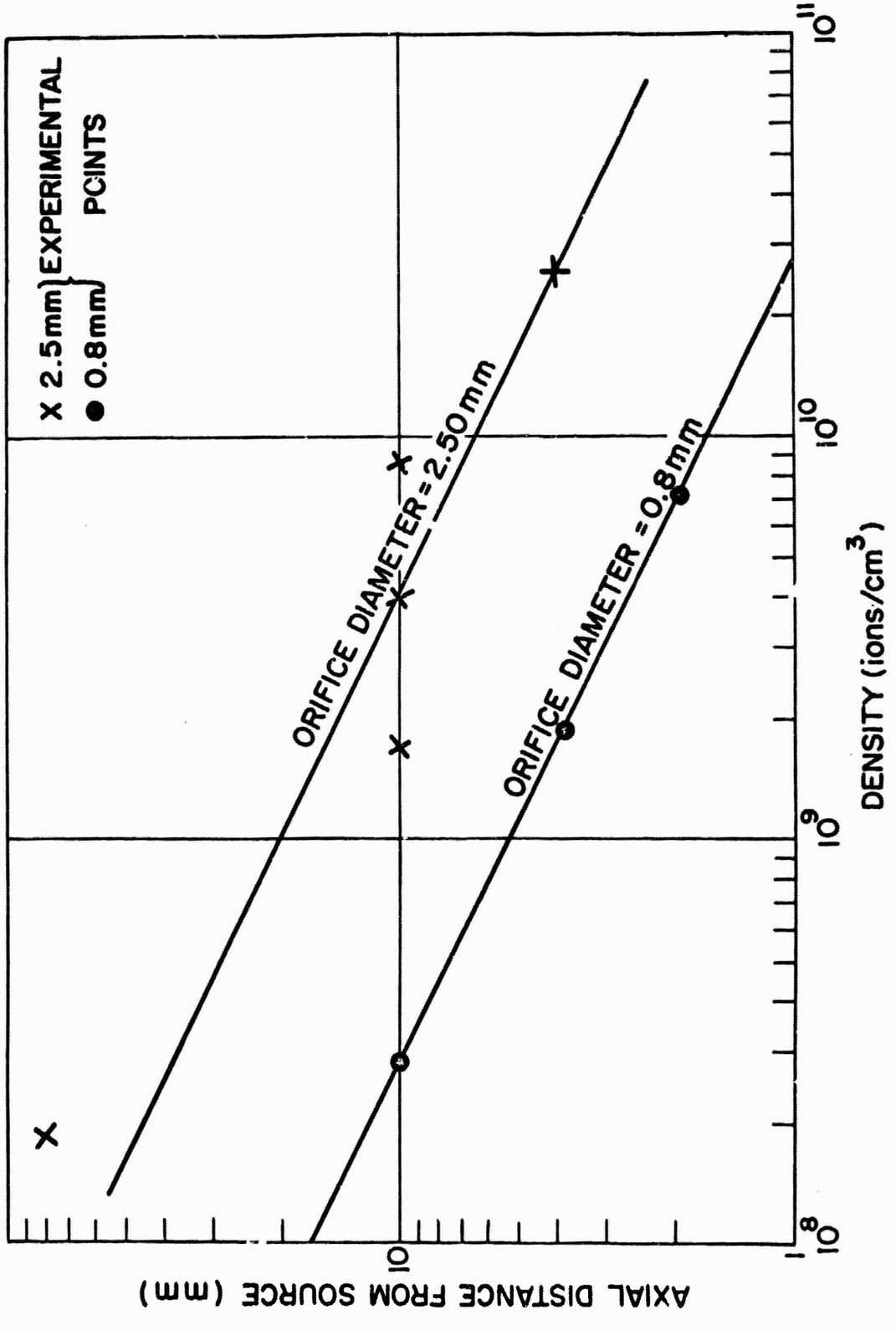

Figure 9. Plasma Density on Axis for Various Apertures

Figure 10. Oscillogram of Ambipolar Diffusion Effect

Ion and electron current to 1st probe as a function of time. Lower curve is electron current.
Horizontal scale: 40μ sec/div.
Vertical scale: electrons - 11 ma/div., ions - 36μ amp/div.
Switching Frequency between ion and electron measurements is 100 KC

Figure 11. Oscillogram of Plasma Velocity (zero rf)

Electron current to 1st and fourth probe as a function of time. Lower curve is current from 1st probe.
Vertical scale: 1st probe - 8.3 ma/div., 2nd probe - 180μ amps/div.
Horizontal scale: 20μ sec/div.

flight of the plasma between two probes, 9 cm apart. The oscillogram in Figure 11 shows the electron current to the two probes as a function of time. The measured plasma ambipolar diffusion velocity was 5×10^5 cm/sec.

The ion temperature T^+ can be calculated from the electron temperature and the plasma velocity. From the theory of ambipolar diffusion as given in Appendix D, the ion temperature is

$$T^+ = -.5\,T^- + \frac{\pi M \bar{v}}{16k}\left[\bar{v} - \sqrt{\bar{v}^2 - \frac{16kT^-}{\pi M}}\right] \qquad (11)$$

in which T^- is the electron temperature, $\bar{v}$ the ambipolar velocity, M the ion mass, and k the Boltzmann constant. For the measured values: $T^- = 20{,}000°K$, $\bar{v} = 5 \times 10^5$ cm/sec, the ion temperature is calculated to be $440°K$.

B. APPLICATION OF 140-MC RF FIELD

1. LARGE SOURCE ORIFICE (2.5 MM DIAMETER)

As reported in the previous semi-annual report, [1] probes were used to measure the plasma velocity with a 140-Mc rf field applied. The primary effect observed was a delay of the main plasma pulse, which arrived at the probe 37 microseconds after the peak discharge in the absence of the rf, and about 53 microseconds after the discharge with 400 volts rf applied.* With the 2.5-mm diameter orifice the electron current from the plasma was observed at a probe 15.5 cm from the source. The plasma pulse delay can be seen in Figure 12, for three different applied rf potentials. This last result demonstrated that the rf field increases the transit time to the probe, i.e., the rf field decelerates the

* A phototube aimed at the plasma source had previously determined that the plasma peak discharge occurs about 10 microseconds after the scope is triggered by the breakdown current.

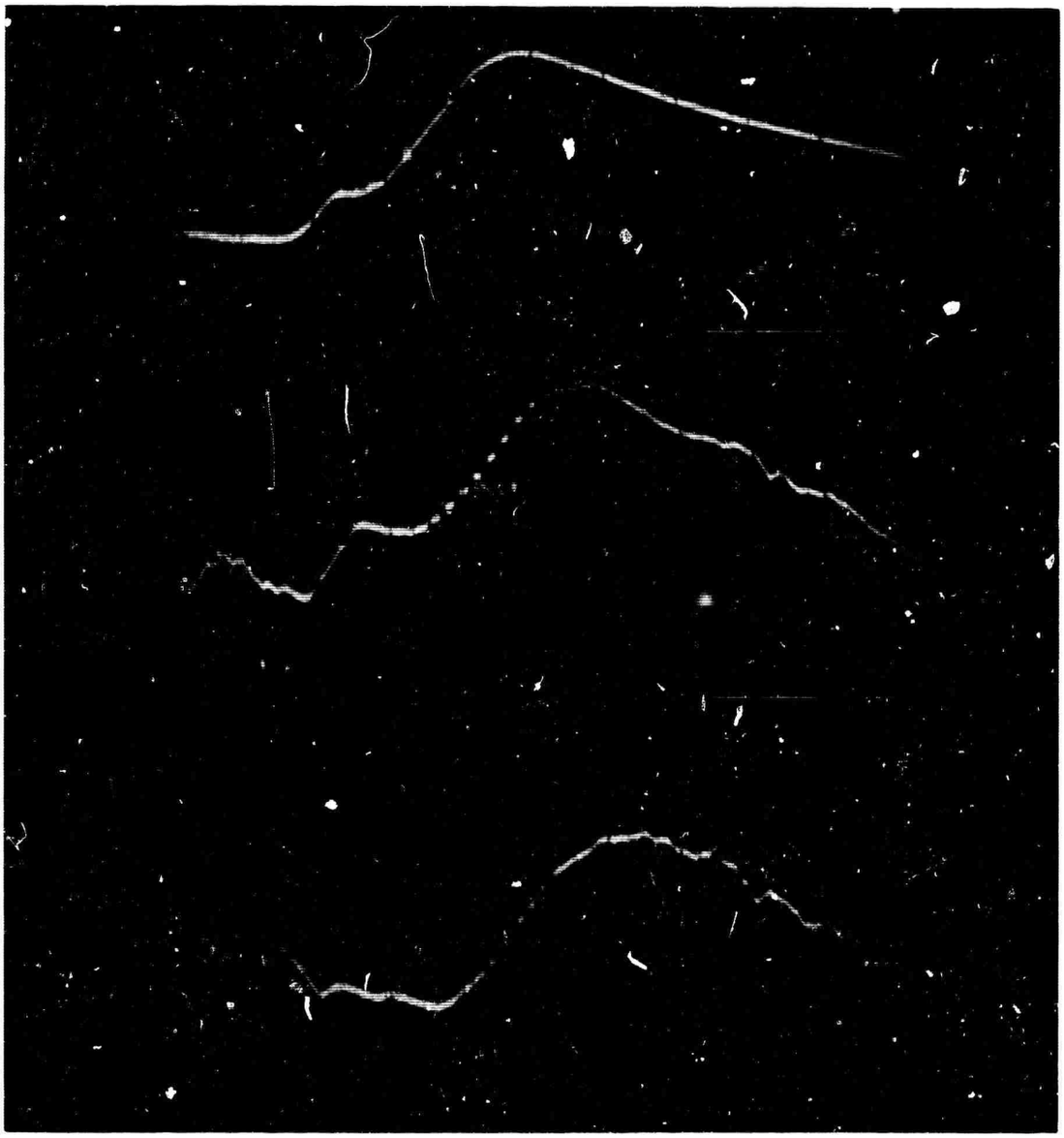

Figure 12. Oscillogram of Plasma Deceleration

Electron current to 2nd probe as a function of time with (a) zero RF potential, (b) 200 volts RF potential, and (c) 400 volts RF potential.
Horizontal scale: 10μ sec div.
Vertical scale: 1.1 ma div.

plasma emerging from the orifice.

The oscillograms in Figure 12 indicate that there is electron current to the probe occurring within one microsecond of the initial discharge and lasting for 20 microseconds. This initial electron current increases with increasing rf field and could not be prevented even when the probe was biased 90 volts negative. This current is presumed to consist of electrons extracted from the plasma and accelerated down the tube by the rf field.

Monitoring of the rf field with a crystal detector while the plasma was in the rf interaction region showed about 25% reduction in field strength due to loading of the rf field by the plasma. However, the field strength was sufficiently high to cause deceleration.

2. SMALL-SOURCE ORIFICE (0.8 MM DIAMETER)

The orifice diameter was decreased to 0.8 mm to reduce the plasma density in the rf interaction region. The plasma was detected by two probes located at 8 cm and 22 cm from the source aperture on the tube axis. The far probe is an aquadag surface painted on the glass.

Figure 13 shows the electron current to the probes as a function of time. Oscillations in each pulse mask the location of the plasma peak, so multiple traces were used to average out these oscillations and permit a time measurement. The final plasma velocity was determined by measuring the plasma transit time between probes. The measured velocity for a maximum rf field amplitude of 76 v/cm was 7×10^5 cm/sec; the velocity increased to 18×10^5 cm/sec when the field amplitude was raised to 136 v/cm. The initial sharp peak, seen in each oscillogram, is an electron pulse which occurs almost simultaneously at each probe.

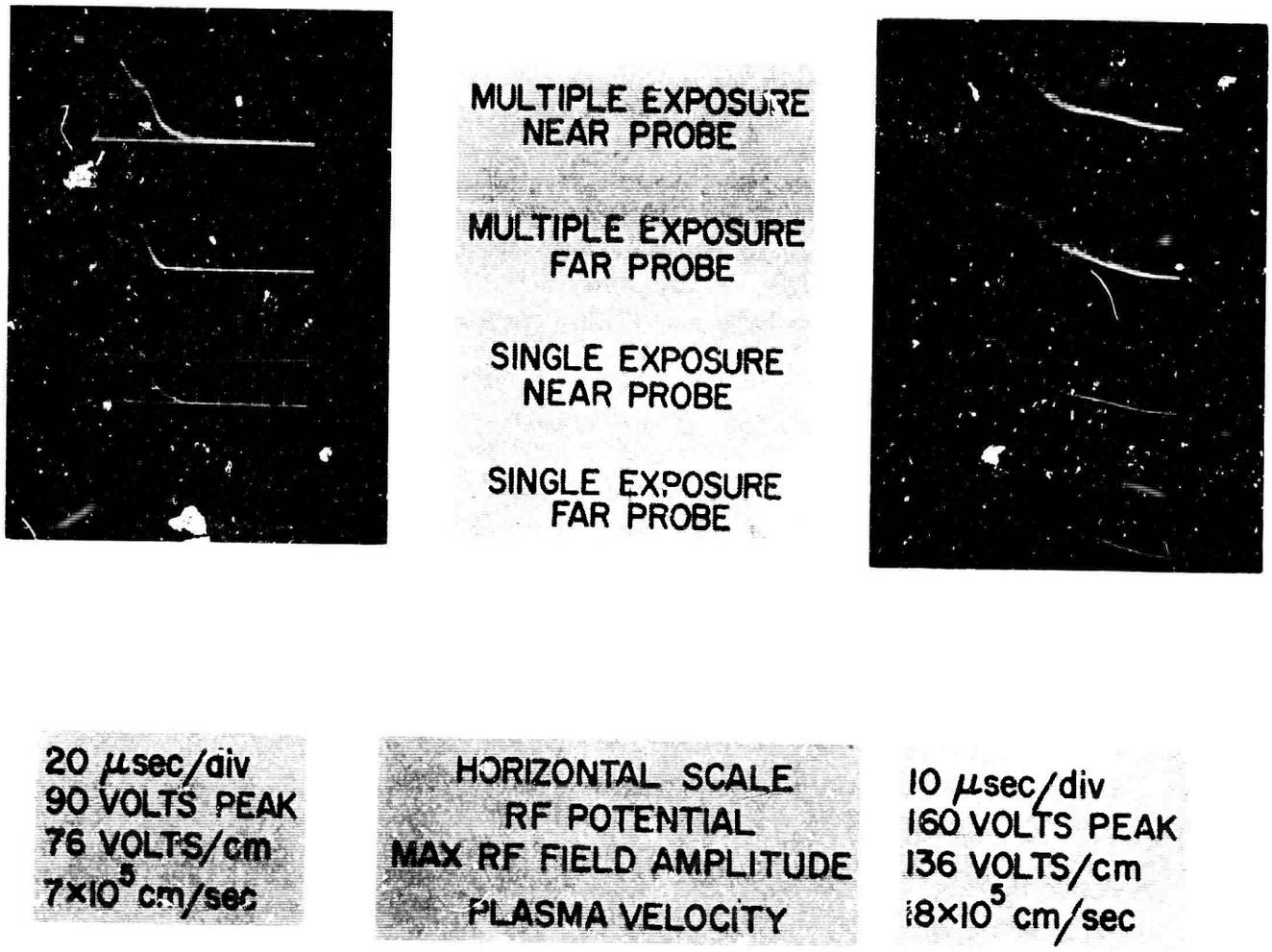

Figure 13. Oscillogram of Plasma Acceleration

A decrease in transit time with increasing rf field was clearly observed; however, the time at which the plasma reaches the near probe is rather uncertain because of oscillations in the detected signal and the large initial electron pulse. Measurements of the time at which the plasma reached the aquadag were less subject to these difficulties. Since the rf field decreases to 1/10 of its maximum value in 3 cm and the acceleration distance is small compared to the total travel distance of 22 cm, the average velocity of the plasma between source and far probe is approximately equal to the final velocity. The time at which the plasma emerges from the orifice is taken to be the time of the initial electron pulse. Average velocities of the plasma from the source to the aquadag surface are plotted as a function of maximum rf field amplitude in Figure 14. The uncertainties in the measurements are indicated by the vertical lines in the figure. There was no measured decrease in rf field as the plasma was being accelerated.

Oscillations of the electron current to the probes can be seen in Figure 13. The frequency of the oscillations is about 200 kilocycles and increases with increasing rf field.

A measurement of the plasma amplitude at various rf fields showed a definite minimum between 0 and 100 volts/cm maximum rf field amplitude as shown in Figure 15. The measurements were made with a probe 12.5 cm from the orifice using a positive bias of 45 volts. The reproduceability of the curve was dependent on the condition and level of the mercury in the igniter source. Discussion and explanation of this effect will be found in section V.

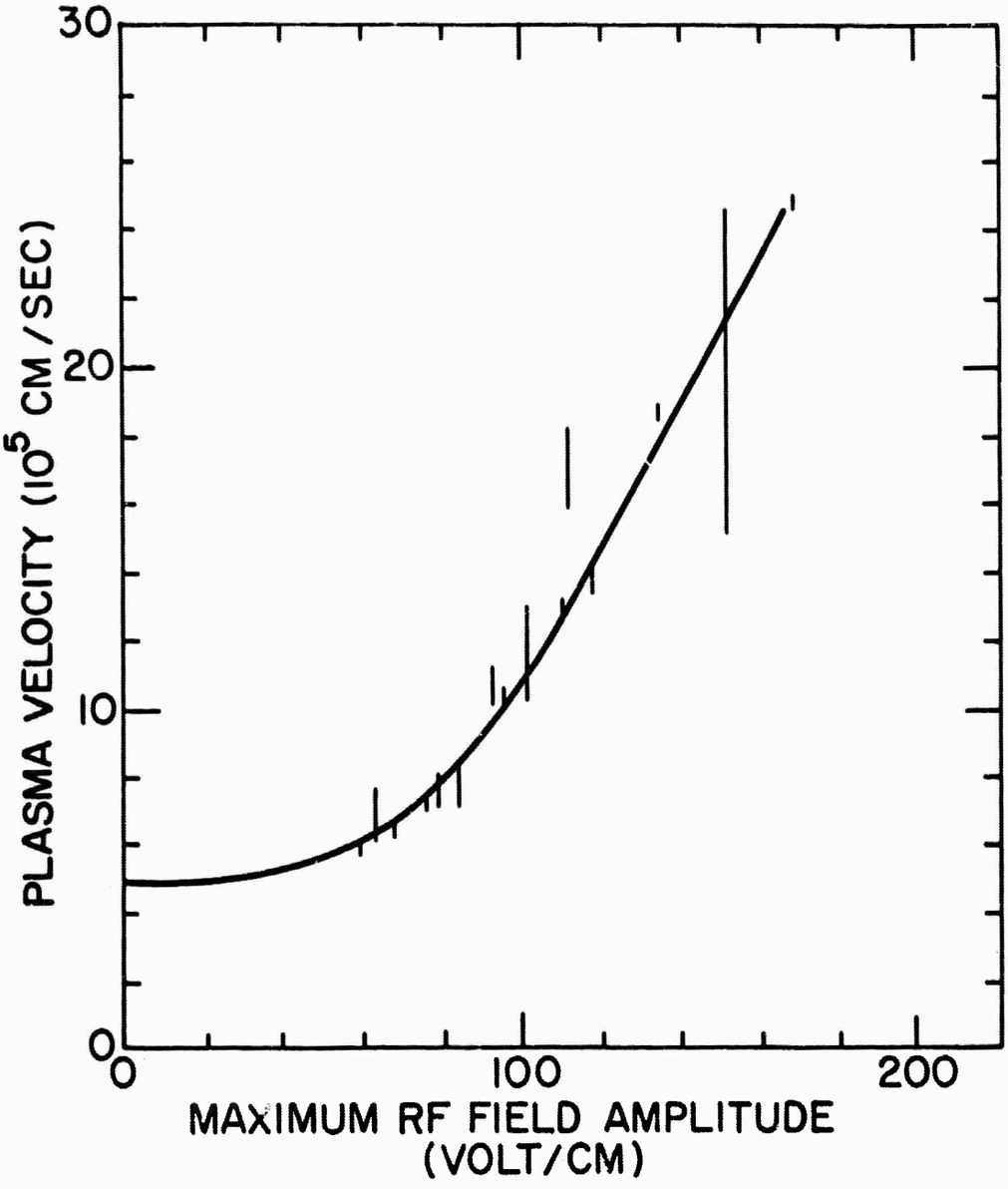

Figure 14. Experimental Plasma Velocities

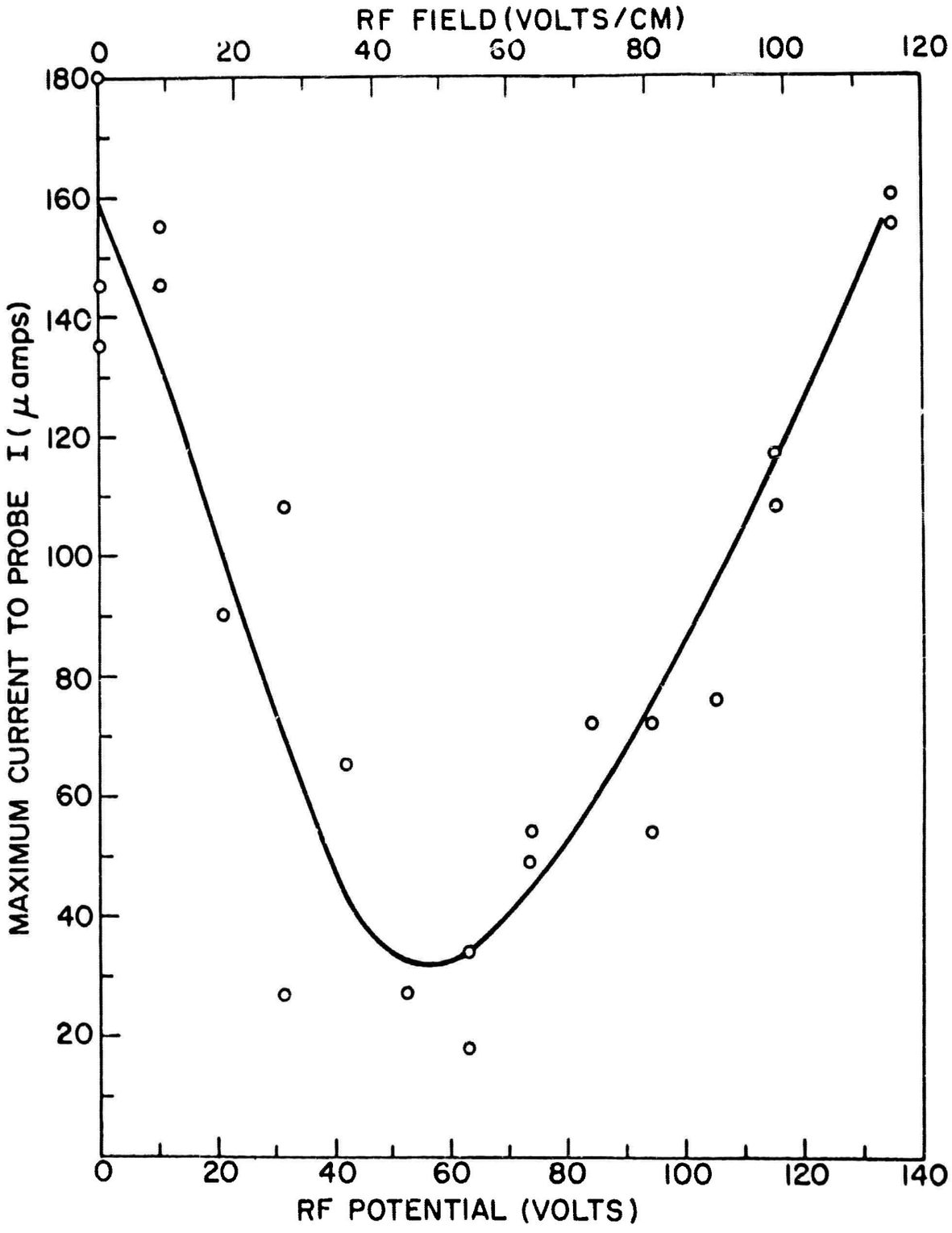

Figure 15. Amplitude Variation of Plasma Pulse with Low rf Fields

V. DISCUSSION

A. COMPARISON OF EXPERIMENTAL RESULTS AND THEORY

1. DECELERATION

When the source orifice was adjusted to a diameter of 2.5 mm and a plasma pulse was produced, deceleration was observed when the 140-Mc rf field was applied. Density measurements, as described in Section IV, show that the plasma emerges with an approximately spherical shape. According to the theory, deceleration will occur in a 140-Mc field for spherically shaped plasma with a density greater that the critical density

$$n_c = 7.5 \times 10^8 \text{ ions/cm}^3 \text{ (from Appendix B } n_c = \frac{3\omega^2 m \epsilon_0}{e^2} \text{)}$$

The density of the plasma emitted from the 2.5-mm-diameter orifice is greater than the critical density in the most effective part of the interaction region. The plasma density decreases to the critical density 2.4 centimeters from the source, the point where the electric field has decreased to 15 percent of maximum. The average velocity to the probe changed from 4.2×10^5 cm/sec. at zero rf to 2.9×10^5 cm/sec. at 340 v/cm rf field. This observed deceleration is in qualitative agreement with the theory. In addition, the substitution of these values in the theoretical expression for final velocity (equation 6) yields a value for density of 5.7×10^9 ions/cm^3. Such a calculated value is consistent with the measured value at a distance of about 8 mm from the source.

2. ACCELERATION

The acceleration predicted by theory has also been observed experimentally. According to the theory, acceleration will occur in a 140-Mc field for a spherically

shaped plasma with the density less than the critical density of 7.5×10^8 ions/cm^3. Plasma densities less than this critical value were obtained with the source orifice of 0.8 mm diameter. Density measurements at the peak of a plasma pulse show that this critical density occurs at a distance of about 0.6 cm from the source. At all greater distances, the density is less than the critical density. At this distance of 0.6 cm, the field has only dropped to 60% of the peak so that a considerable portion of the plasma is in an accelerating field and thus acceleration is expected. The velocity was observed to increase from 5×10^5 cm/sec at zero rf field to 25×10^5 cm/sec at an rf field of 170 v/cm.

3. PLASMA VELOCITY VERSUS RF FIELD

The velocity that was obtained experimentally using an orifice of 0.8 mm diameter is plotted against rf field in Figure 16. Also plotted are theoretical curves for values of the operating frequency of 1.05 and 1.025 times the critical frequency, with an assumed initial velocity equal to the measured value.

The observed velocity increases with field, in qualitative agreement with the theory. To obtain the high velocities observed with the magnitude of field used, theory requires that the critical frequency for the plasma be very close to the applied frequency. The fact that best agreement exists for a value of ω_c/ω so near to 1 suggests that either an internal mechanism exists for assisting the resonance or that only that portion of the plasma with the critical density is accelerated. In either case, such an effect may be exploited in future experiments to shift from a pulsed to a continuous type of source.

The discrepancy between the observed and theoretical slopes may be attributed to theoretical assumptions, experimental errors, or a change in plasma characteristic as the field changes. Theoretical assumptions that the plasma originates at the rf field maximum and that the plasma density is uniform were not realized in practice. A change in plasma characteristic due to focusing by the radial field gradient, shown in Figure 6, may increase the plasma density, and thus the

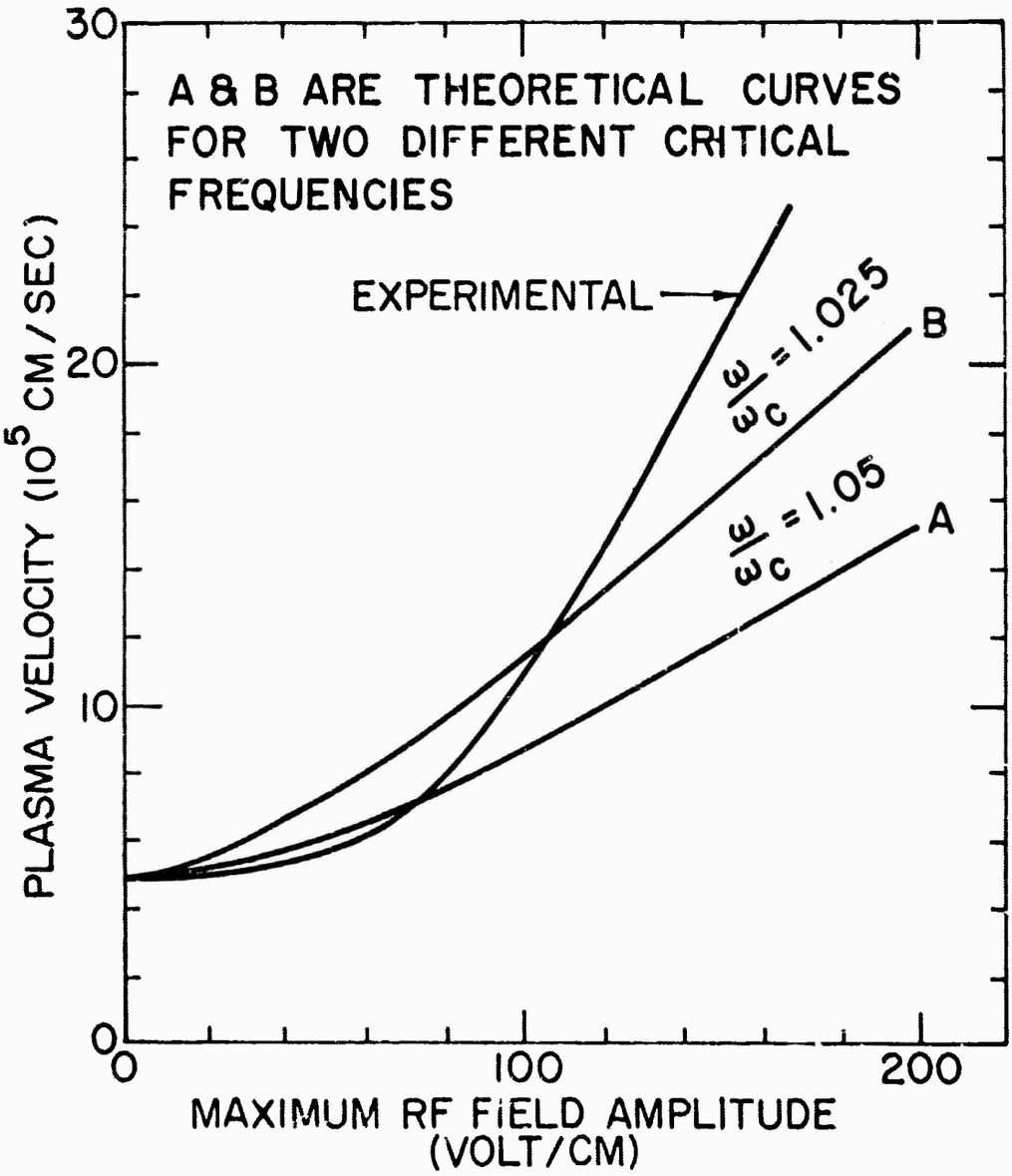

Figure 16 Comparison of Experimental and Theoretical Plasma Velocities

increased slope would be expected because of the decrease in the ratio of ω/ω_c.

B. OSCILLATIONS IN PROBE SIGNALS

For an accelerated plasma, oscillations with a period of about 5 microsecond were observed in the probe signals. The oscillation frequency increased with increasing applied field. With the larger orifice, when the plasma was decelerated, this type of oscillation was not observed.

There are several possible explanations for these oscillations:

(1) Plasma having a density well below the critical density will not be appreciably accelerated by the rf field gradient. Thus plasma emerging from the source must approach a density close to the critical density before acceleration takes place. This plasma is accelerated leaving behind a plasma void. More plasma moves from the source into the void and the process is repeated. The frequency of this cyclic process is dependent on the plasma diffusion velocity.

(2) If there is an axial field gradient there must be a radial field gradient. When the plasma density is almost equal to the critical density the plasma will be strongly focused by the radial gradient. The focusing will produce a pinching effect so that the plasma would emerge from the rf interaction region as individual plasma puffs.

(3) Acceleration of the plasma results in a leading negative space charge region (electrons) and a trailing positive space charge region (ions). Plasma moving in behind the accelerated plasma sees the positive space charge region. The ions are repelled and space charge density fluctuations may be established.

Oscillations of the above type have also been observed in experiments with thermionic converters containing cesium plasma.[17] In the latter case, it

has been shown that these oscillations arise from an instability in the plasma potential.

C. VARIATION OF PROBE SIGNAL AMPLITUDE

At rf field levels below 120 v/cm, the probe signal varies in an interesting and explainable manner. As shown in Figure 15, the amplitude of the probe electron current as a function of rf field exhibits a minimum at 45 v/cm.

To explain these results, it is necessary to observe that the plasma does not start at a point of maximum field, as assumed by the theory, but starts inside the igniter source at a point of zero field. For very low rf voltages the plasma is decelerated until it reaches the maximum field point, and then accelerated. As the rf voltage is increased, some of the plasma will not have enough initial kinetic energy to overcome this deceleration, and will be turned back before it reaches the maximum field point. For fields higher than about 45 v/cm, electrons can be accelerated all the way to the maximum field point in less than one rf cycle and are not contained by the field barrier. Hence the number of electrons observed increases for higher rf fields. The oscillation amplitude for electrons in a 140-Mc field of 45 v/cm is about 1.0 mm, which is also the distance between the maximum field point and a point in the orifice where the field is negligible. Therefore the magnitude of the rf field for which the minimum amplitude is observed is in good agreement with the theory.

Appendix E contains a more detailed theoretical treatment of this effect.

D THRUST CALCULATIONS

Calculations show that the thrust $(MN_c v^2)$ from the system at the peak of a pulse is about 0.13 dynes/cm^2. Since the duty cycle is extremely small, the

average thrust is too small for measurement and a detector with both sufficiently high-frequency response and sensitivity to measure the transient thrust is not available.

For measurement purposes, the average thrust must be increased significantly. A larger thrust can be obtained by increasing the plasma density and increasing the driving frequency correspondingly. The average thrust can also be increased by using a faster pulse rate or a continuous source instead of the present low duty cycle. The increased duty cycle in conjunction with a higher density plasma should produce sufficient thrust to be detected by mechanical means and the results of such experiments would provide additional data for comparison with the theory.

E. ENERGY OF ACCELERATED IONS

The high translational energy achieved by the ions is noteworthy. This high ion energy has been observed both in the ambipolar diffusion mechanism and in acceleration by an rf field gradient. In the ambipolar diffusion experiments, where the ion acceleration is caused by the pull of the high speed thermal electrons, the ion velocity was 5×10^5 cm/sec. This velocity is equivalent to an energy of 25 volts. In the case of the rf field gradient acceleration, a maximum rf potential of only 200 volts was applied and the velocity of the plasma was increased to 25×10^5 cm/sec., equivalent to an ion energy of 625 volts. During the acceleration period, electrons must transfer the energy they abstract from the field to ions quite rapidly.

VI. CONCLUSIONS AND PLANS

A. MAJOR ACCOMPLISHMENTS

During the first six months of this study, theoretical analyses predicted that rf forces may be directed toward the field maximum as well as away from it and experimental results demonstrated a change in magnitude of the plasma velocity due to the rf field. During the second six months, the theory was extended from a two particle model to one based on macroscopic plasma properties. The new theory yields the same final result as the earlier theory and in addition permits calculations of acceleration for more realistic plasma shapes than the earlier assumed infinite slab. Experimental results have demonstrated both the acceleration and deceleration of a plasma in accordance with the theoretical predictions.

B. SOME DETAILS OF THE ACCOMPLISHMENTS

Calculations for the acceleration of plasma spheres and ellipsoids with any orientation with respect to the rf field have been completed. These show that accelerations of plasmas with a density higher than that in a slab are possible for a specific rf frequency. In particular, for a 10-to-1 length-to-width ratio in an ellipsoid, the density at which the direction of force changes is fifty times that for a plasma slab. Hence, for a given rf frequency, use of such a needle-shaped plasma could allow acceleration of plasma of density fifty times larger than is possible with a plasma slab.

A reliable plasma source was developed. This source permits the density of the plasma entering the interaction region to be varied by adjusting the source aperture. Plasma density contours were determined in the interaction region near the orifice for various orifice sizes. Probes have been used to detect the moving plasmas and to determine plasma transit times. Plasma has been accelerated to a

velocity of 25 x 10^5 cm/sec which is equivalent to a specific impulse of 2500 seconds. Low-density plasmas were accelerated and high-density plasmas were decelerated as predicted by theory. The variations in plasma velocity and probe signal amplitude with changes in rf field magnitude were compared to and explained by the theory.

C. FUTURE WORK

To provide a quantitative test of the theory, the dependence of the acceleration on the applied frequency will be determined. Higher frequencies will permit the use of higher density plasmas; this should result in thrusts of sufficient magnitude to be detected experimentally. Measurements at 300 Mc are in progress. The construction of a 2.5 kMc system is planned. The increased plasma densities for use with this high-frequency system should be available from a source of design similar to that used at lower frequencies.

The igniter source will be provided with an electronic shutter to define the plasma pulse shape more sharply. A sharply defined plasma pulse should assist in improving the accuracy of velocity measurements.

Requirements of a continuous operation system rather than a pulsed one will be investigated. With experimental information from the work at various frequencies, specific impulse, thrust, density and optimum frequency will be determined.

Theoretical studies of the properties of plasmas in rf field gradients will be continued. Interpretations of the experimental results at higher frequencies and densities will be made. The theory for the acceleration of non-uniform plasma is being developed.

APPENDIX A

EFFECT OF DC BIAS

This section discusses the effect of dc bias on rf acceleration. It is assumed that a dc potential is applied on the same electrodes as is the rf; hence, the rf and dc field distributions are the same. The analysis is similar to the calculations for rf alone,[1] and the same basic assumptions are made. A fully ionized plasma of constant density in the form of an infinite slab perpendicular to the rf field is assumed. It is further assumed that the plasma slab continues as a rigid plasma slab. The latter assumption may be even less justified for dc than it is for rf; nevertheless, the theory yields some interesting results.

The major effect of a dc bias is to change the effective plasma resonant frequency. The applied frequency at which the acceleration changes sign is greater if the gradient of the dc field is positive, and less if the gradient is negative. To decrease the effective plasma resonance the center electrode should therefore have a positive charge.

Before proceeding to the theory, it may be useful to visualize the process that changes the frequency. Consider a plasma slab with no applied fields. The electron potential energy can be calculated for various positions of the electron center of mass. If the electrons are displaced from their equilibrium positions an oscillation will take place, the frequency being determined by the curvature of the potential energy curve and the mass of the electrons. If a uniform dc field is applied, the equilibrium position of the electrons is changed, corresponding to the polarization of the plasma, but the resonant frequency remains constant, as shown in Figure 17. If a dc field gradient is applied, a curved potential is added, which changes the curvature of

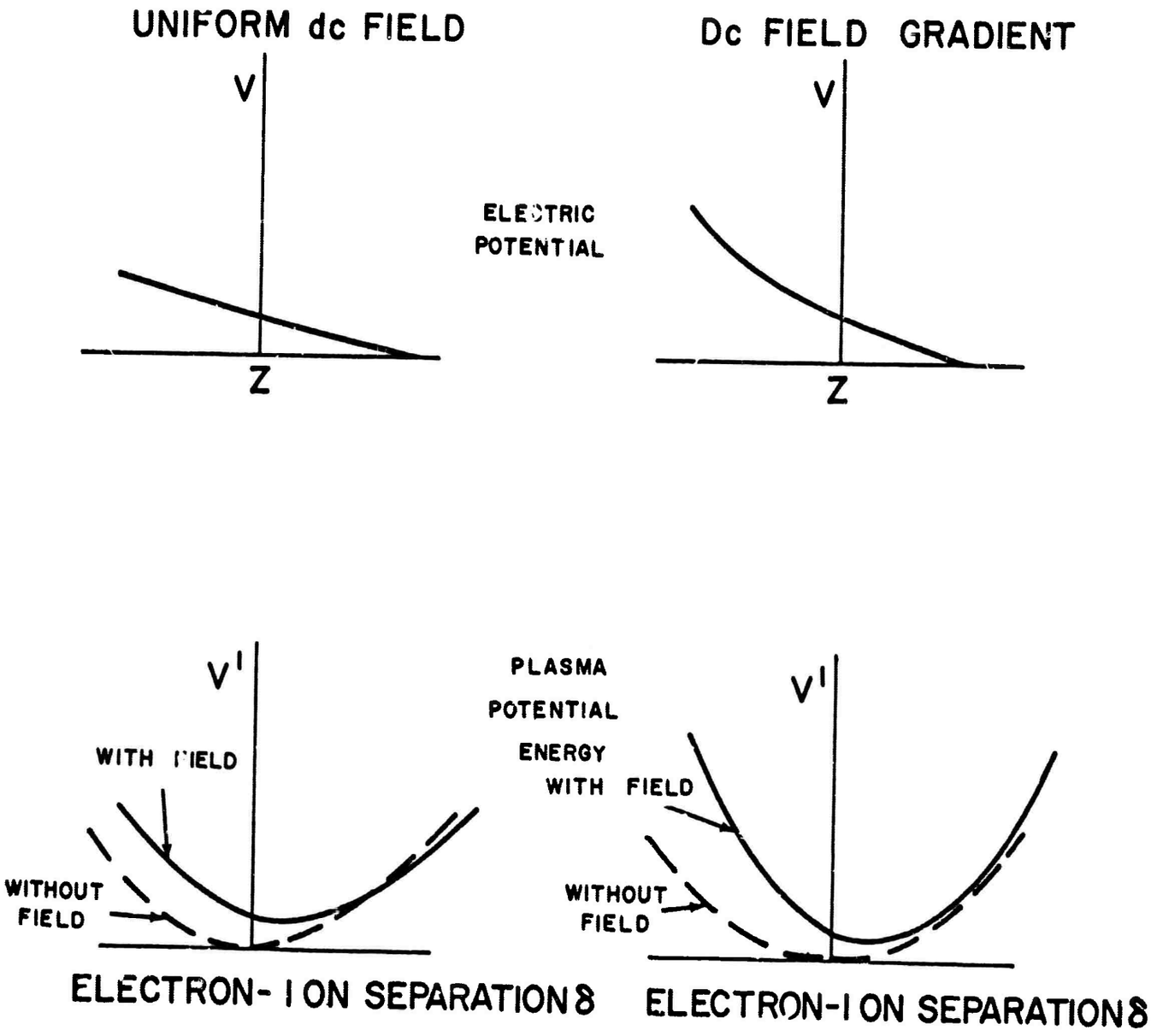

Figure 17. Change in Plasma Frequency by D.C. Field Gradient

the potential energy curve and hence changes the resonant frequency, as shown in Figure 17.

The differential equations of motion for the plasma center of mass Z_m and the separation δ between the ion and electron center of masses are[1]:

$$\frac{d^2 Z_m}{dt^2} = -\frac{e}{M}\,\delta\,\frac{\partial E}{\partial Z} \tag{A-1}$$

$$\frac{d^2\delta}{dt^2} + \nu\,\frac{d\delta}{dt} + \omega_p^{\,2}\,\delta + \frac{e}{m}\,\frac{\partial E}{\partial Z}\,\delta = -\frac{e}{m}\,E \tag{A-2}$$

E is the applied field and $\frac{\partial E}{\partial Z}$ is the applied field gradient at Z_m ; ν is the electron collision frequency, ω_p the plasma frequency, e and m the electron charge and mass, and M is the ion mass.

The applied field consists of an rf voltage and a dc bias, and can be written in the form

$$E = E_{rf}\,cos\omega t + E_{dc} \tag{A-3}$$

The result of substituting equation (3) into equation (2) is

$$\frac{d^2\delta}{dt^2} + \nu\,\frac{d\delta}{dt} + \omega_p^{\,2}\,\delta + \frac{e}{m}\left(\frac{\partial E_{rf}}{\partial Z}\right)\delta\,cos\omega t + \frac{e}{m}\left(\frac{\partial E_{dc}}{\partial Z}\right)\delta = \tag{A-4}$$

$$-\frac{e}{m}\,E_{rf}\,cos\omega t - \frac{e}{m}\,E_{dc}$$

It is convenient to define the following quantities: *

$$\omega_g^2 \equiv \frac{e}{m} \frac{\partial E_{rf}}{\partial Z} \tag{A-5}$$

$$\delta' \equiv \delta + \frac{e}{m} \frac{1}{\omega_p'^2} E_{dc} \tag{A-6}$$

$$\omega_p'^2 = \omega_p^2 + \frac{e}{m} \frac{\partial E_{dc}}{\partial Z} \tag{A-7}$$

$$E'_{rf} = E_{rf} - \frac{\omega_g^2}{\omega_p'^2} E_{dc} \tag{A-8}$$

The result of substituting the above quantities into equation (A-4) is to eliminate the constant term on the right hand side:

$$\frac{d^2\delta'}{dt^2} + \nu \frac{d\delta'}{dt} + \omega_p'^2 \delta' + \omega_g^2 \delta' \cos\omega t = -\frac{e}{m} E'_{rf} \cos\omega t \tag{A-9}$$

The equation is now in the same form as the equation in the theory without the dc bias, and can be solved by similar methods. Neglecting the fourth terms (if $\omega_g^2 \ll \omega_p'^2$), the steady state solution of equation (A-9) is

$$\delta' = -\frac{e}{m} E'_{rf} \frac{\cos(\omega t - \phi)}{[(\omega_p'^2 - \omega^2)^2 + (\omega\nu)^2]^{1/2}} \tag{A-10}$$

---

*Note that equation (A-6) merely separates out the average plasma separation which is the polarization produced by the dc field. Similarly equation (A-7) expresses the change in plasma resonance frequency due to the dc field. The latter equation is somewhat more symmetrical if the electron mass is not negligible compared to the ion mass, in which case the resonance frequency is given by:

$$(\omega_p'')^2 = \frac{Ne^2}{\epsilon_o} \frac{M+m}{Mm} + \frac{e(M-m)}{Mm} \frac{\partial E_{dc}}{\partial Z}$$

so that the dc bias effect vanishes if the masses of the positively charged particles equals that of the negatively charged particles.

where

$$\tan \phi = \frac{\omega \nu}{\omega_p'^2 - \omega^2} \tag{A-11}$$

Combining equations (A-1), (A-3), (A-6) and (A-8), the instantaneous acceleration of the particle center of mass is

$$\frac{d^2 Z_m}{dt^2} = -\frac{e}{M}\left[\frac{\partial E_{rf}}{\partial Z}\cos\omega t + \frac{\partial E_{dc}}{\partial Z}\right]\left\{-\frac{e}{m}\frac{E_{dc}}{\omega_p'^2} - \frac{e}{m}E_{rf}\frac{\cos(\omega t-\phi)}{[(\omega_p'^2-\omega^2)^2+(\omega\nu)^2]^{1/2}}\right\} \tag{A-12}$$

The average acceleration is therefore

$$\left\langle \frac{d^2 Z_m}{dt^2} \right\rangle_{AV} = \frac{e^2}{mM}\frac{E_{dc}}{\omega_p'^2}\frac{\partial E_{dc}}{\partial Z} + \frac{e^2}{2mM}\left[E_{rf} - \frac{\omega_g^2}{\omega_p'^2}E_{dc}\right]\frac{\partial E_{rf}}{\partial Z}\frac{\omega_p'^2 - \omega^2}{[(\omega_p'^2-\omega^2)^2+(\omega\nu)^2]} \tag{A-13}$$

The first term is simply the acceleration towards the maximum of an electric field that any dielectric experiences.

If

$$\frac{E_{rf}}{E_{dc}} >> \left(\frac{\omega_g}{\omega_p'}\right)^2 \tag{A-14}$$

$$\omega^2 = \omega_p^2 + \omega_p'\nu = \text{the square of the frequency which maximizes the acceleration} \tag{A-15}$$

and

$$\omega_p' >> \nu \tag{A-16}$$

then

$$\left\langle \frac{\partial^2 Z_m}{\partial t^2} \right\rangle = \frac{e^2}{2mM\omega_{p'}^2} \left\{ \nabla E_{dc}^2 - \frac{\omega_{p'}}{4\nu} \nabla E_{rf}^2 \right\} \tag{A-17}$$

$$\sim -\frac{e^2}{8mM\nu\omega_{p'}} \nabla E_{rf}^2$$

Thus it has been shown that the average acceleration is in the same form as the theoretical result without the dc bias, except for the change in plasma resonant frequency. If the bias is increased too far, the terms which were neglected would become important, and the acceleration would be towards the field maximum.

APPENDIX B

ACCELERATION OF PLASMA ELLIPSOIDS

The theory presented in the text on the acceleration of a plasma slab in an rf field gradient can be extended to include the acceleration of a plasma ellipsoid. The theory will then include the slab as a special case, as well as most other cases of interest. The energy of a dielectric ellipsoid is calculated, with the dielectric constant that of the plasma. The force on the plasma can then be obtained by differentiating the potential energy with respect to position, or the final velocity achievable can be calculated by equating the potential energy to kinetic energy. As before, it is assumed that the plasma is fully ionized, of constant density, and that it is in a quasistatic electric field which is approximately uniform over the distance the plasma moves during one rf cycle. It is also assumed that the shape of the ellipsoid is unaffected by the accelerating forces.

The dielectric ellipsoid is assumed to have semi-principal axes of length $a, b, c,$ oriented along the x, y, z axes respectively, and a dielectric constant K. The potential energy of the ellipsoid is then [18]

$$U = -\frac{1}{4}(K-1)\epsilon_o \left\{ \frac{E_{ox}^2}{1+\frac{abc}{2}(K-1)A_1} + \frac{E_{oy}^2}{1+\frac{abc}{2}(K-1)A_2} + \frac{E_{oz}^2}{1+\frac{abc}{2}(K-1)A_3} \right\} \qquad \text{(B-1)}$$

where E_o is the amplitude of the applied rf field and where

$$A_1 = \int_o^\infty \frac{ds}{(s+a^2)R_s} \qquad A_2 = \int_o^\infty \frac{ds}{(s+b^2)R_s}$$

$$A_3 = \int_o^\infty \frac{ds}{(s+c^2)R_s} \qquad \text{where} \quad R_s = \sqrt{(s+a^2)(s+b^2)(s+c^2)} \qquad \text{(B-2)}$$

The dielectric constant of plasma of constant density is given by [15]

$$K-1 = \frac{\omega_p^2}{-\omega^2 + j\omega\nu} \tag{B-3}$$

This dielectric constant is substituted into Equation B-1, and the real part of U is calculated. If this energy is converted to translational energy the final velocity for a plasma in a field-free region, which had an initial velocity v_i in an electric field E_o is

$$v_f^2 = v_i^2 + \frac{e^2}{2mM}\left\{\frac{\omega^2-\omega_1^2}{(\omega^2-\omega_1^2)^2+(\omega\nu)^2}E_{ox}^2 + \frac{\omega^2-\omega_2^2}{(\omega^2-\omega_2^2)^2+(\omega\nu)^2}E_{oy}^2 + \frac{\omega^2-\omega_3^2}{(\omega^2-\omega_3^2)^2+(\omega\nu)^2}E_{oz}^2\right\} \tag{B-4}$$

where

$$\omega_1^2 = \omega_p^2\frac{abc}{2}A_1 \qquad \omega_2^2 = \omega_p^2\frac{abc}{2}A_2$$

$$\omega_3^2 = \omega_p^2\frac{abc}{2}A_3 \qquad \omega_p^2 = \frac{ne^2}{m\epsilon_o} \tag{B-5}$$

A plasma ellipsoid with unequal axes has three main resonant frequencies. Other frequencies may be excited if the applied electric field is not uniform. It is useful to note a simple relation between these frequencies, namely that the sum of the squares is equal to square of the resonant frequency for a slab, i.e.,

$$\omega_p^2 = \omega_1^2 + \omega_2^2 + \omega_3^2 \tag{B-6}$$

This can be proved by an integration by parts of A_1. For a plasma sphere the three frequencies are equal, therefore the resonant frequency of a sphere is

$$\omega_c^2 = \frac{ne^2}{3m\epsilon_o} \tag{B-7}$$

The actual resonant frequency in general cannot be written in analytical form, since the integration is not possible. However, special cases can be evaluated, and a number of them are presented in Table B-1. Included is the case of a plasma slab, which has a higher resonant frequency than any of the other cases. Of special interest

TABLE B-1

RESONANT FREQUENCIES FOR PLASMA ELLIPSOIDS

Plasma Shape	Relation of axes	$\omega_1^2 / \omega_p^2 = \frac{abc}{2} \int_0^\infty \frac{ds}{(s+a^2)^{3/2}(s+b^2)^{1/2}(s+c^2)^{1/2}}$
Slab ($\perp$ to field)	$b \to \infty \quad c \to \infty$	1
Sphere	$a=b=c$	$1/3$
Elliptic cylinder ($\parallel$ to field)	$a \to \infty$	0
Slab ($\parallel$ to field)	$a \to \infty \quad c \to \infty$	0
Elliptic cylinder ($\perp$ to field)	$a \to \infty$	$\frac{b}{a+b}$
Oblate spheroid ($\parallel$ to field)	$c=b \quad b > a$	$\frac{r^2}{r^2-1} \left\{ 1 - \frac{\sec^{-1} r}{\sqrt{r^2-1}} \right\}$
Prolate spheroid ($\parallel$ to field)	$c=b \quad b < a$	$\frac{b^2/a^2}{e^3} \left\{ -e + \frac{1}{2} \ln \frac{1+e}{1-e} \right\}$
Oblate spheroid ($\perp$ to field)	$c=a \quad b < a$	$\frac{r/2}{1-r^2} \left\{ -r + \frac{\cos^{-1} r}{\sqrt{1-r^2}} \right\}$
Prolate spheroid ($\perp$ to field)	$c=a \quad b > a$	$\frac{1}{2f^2} \left\{ -\frac{b^2}{a^2} + \frac{1}{2f} \ln \frac{1+f}{1-f} \right\}$

where

$$r = b/a \qquad e = \sqrt{1-(b^2/a^2)} \qquad f = \sqrt{1-(a^2/b^2)}$$

is the geometry with axial symmetry, where the electric field is along the symmetry axis. The resonant frequency is plotted in Figure 19 as a function of the ratio of the third axis to the other two.

For comparison to theories of plasma confinement, the mechanical force exerted on the plasma can be obtained by calculating the variation of the potential energy U with respect to a small displacement. The force on the plasma $\underline{f}$ is equal to

$$\underline{f} = -\nabla U =$$

$$\frac{ne^2}{4m}\left\{\frac{\omega^2-\omega_1^2}{(\omega^2-\omega_1^2)^2+(\omega\nu)^2}\nabla E_{ox}^{\,2}+\frac{\omega^2-\omega_2^2}{(\omega^2-\omega_2^2)^2+(\omega\nu)^2}\nabla E_{oy}^{\,2}+\frac{\omega^2-\omega_3^2}{(\omega^2-\omega_3^2)^2+(\omega\nu)^2}\nabla E_{oz}^{\,2}\right\} \qquad \text{(B-8)}$$

A conclusion from this analysis is that acceleration of other plasma geometries is very similar to that of a plasma slab; the principal difference is in the relationship between the resonant frequency and the plasma density. For acceleration to a field-free region it is necessary that the applied frequency be above the resonant frequency; thus to accelerate a high-density plasma it is desirable to have it assume a shape such as to minimize its resonant frequency. The most important conclusion of the theory presented is that for a long needle of plasma, parallel to the rf field, the resonant frequency decreases rapidly as the length to width ratio increases. In particular, as seen in Figure 18, for a 10-to-1 length-to-width ratio, the critical density is fifty times that for a plasma slab. Use of such a needle-shaped plasma could allow acceleration of plasma of density fifty times larger than is possible with a slab of plasma, provided that the assumption of a constant shape can be satisfied.

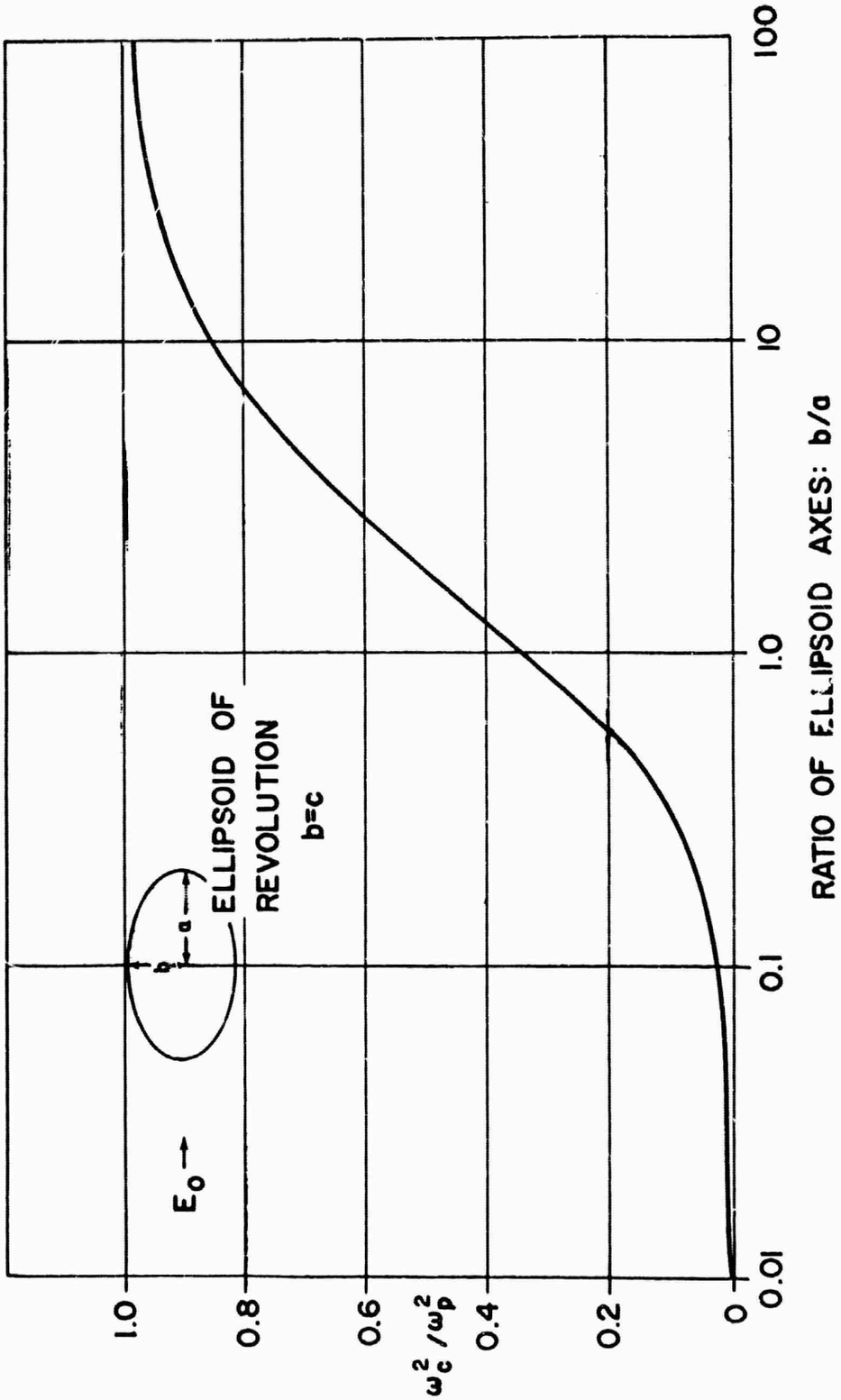

Figure 18. Critical Frequency for Plasma Ellipsoids

BLANK PAGE

APPENDIX C

EFFECT OF LARGE FIELD GRADIENTS

Theoretical calculations of the plasma acceleration by rf have been made for small field gradients. In the theory based on energy considerations the motion of the center of mass of the plasma was assumed to be small in each period of the rf field. In the original mathematical formulation,[1] ω_g^2 is assumed small compared to ω_p^2, where $\omega_g^2 \equiv e/m \ \frac{\partial E}{\partial Z}$. Such an approximation is useful in understanding plasma acceleration.

The present equipment is capable of rf voltages high enough so that $\omega_g > \omega_p$. However, when such voltages are applied, the observed plasma oscillations prevent any transit time measurements. For this reason most experiments have been performed below this limit. Fundamental changes are observed when the field gradient approaches this limit. These changes alter the nature of the acceleration. In an effort to understand these changes an harmonic analysis that includes the fundamental frequency and the first harmonic but neglects higher frequency terms has been performed. The results provide some insight into changes that occur as the limit is approached, but are not valid for $\omega_g > \omega_p$.

The plasma is assumed to be made up of two rigid slabs of ions and electrons, and the differential equations to be solved are [1]

$$\frac{d^2\delta}{dt^2} + \nu \frac{d\delta}{dt} + \omega_p^2 \, \delta + \omega_g^2 \, \delta \cos(\omega t + \phi) = -\frac{e}{m} |E| \cos(\omega t + \phi) \qquad \text{(C-1)}$$

$$\frac{d^2 Z_m}{dt^2} = -\frac{m}{M} \omega_g^2 \, \delta \cos(\omega t + \phi) \qquad \text{(C-2)}$$

where the plasma is assumed to be in a localized region with the center of mass at Z_m and the rf field magnitude is $|E|$.

According to Equation C-2, the average acceleration of the plasma during one period of the rf is

$$\left\langle \frac{d^2 Z_m}{dt^2} \right\rangle_{AV} = - \frac{m}{M} \omega_g^2 \left\langle \delta \cos(\omega t + \phi) \right\rangle_{AV} \qquad \text{(C-3)}$$

To calculate the right hand side, it is necessary to obtain the separation δ. If δ is expressed as a Fourier series, the only component that is important is that of fundamental frequency, since the other components will disappear when the average of Equation C-3 is taken.

The separation δ is assumed to be in the form

$$\delta = \frac{e}{m} |E| \left\{ A \frac{1}{\omega_g^2} + B \cos\omega t + C \cos(2\omega t + \phi + \psi) \right\} \qquad \text{(C-4)}$$

where the phase of the fundamental frequency is included in the phase factor in the differential equations. Equation C-4 is now substituted into Equation C-1, and the collection of terms leads to the five equations

$$\text{Constant:} \quad A \frac{\omega_p^2}{\omega_g^2} + B \omega_g^2 \frac{\cos\phi}{2} = 0 \qquad \text{(C-5)}$$

$$\cos\omega t: \quad A\cos\phi + B(\omega_p^2 - \omega^2) + C\omega_g^2 \frac{1}{2} \cos\psi = -\cos\phi \qquad \text{(C-6)}$$

$$\sin\omega t: \quad -A\sin\phi - B\nu\omega - C\omega_g^2 \frac{1}{2} \sin\psi = \sin\phi \qquad \text{(C-7)}$$

$$\cos 2\omega t: \quad B\omega_g^2 \frac{1}{2}\cos\phi + C(\omega_p^2 - 4\omega^2)\cos(\phi+\psi) - C\,2\nu\omega\sin(\phi+\psi) = 0 \qquad \text{(C-8)}$$

$$\sin 2\omega t: \quad -B\omega_g^2 \frac{1}{2}\sin\phi - C(\omega_p^2 - 4\omega^2)\sin(\phi+\psi) - C\,2\nu\omega\cos(\phi+\psi) = 0 \qquad \text{(C-9)}$$

while the higher frequency term ($3\omega t$) is dropped. These five equations can be solved for the five quantities A, B, C, ϕ, and ψ.

The result of solving Equation (C-8) and (C-9) for ψ and B/C is

$$\tan \psi = - \frac{2\omega\nu}{\omega_p^2 - 4\omega^2} \tag{C-10}$$

$$B/C = -2r/\omega_g^2 \tag{C-11}$$

where

$$r = [(\omega_p^2 - 4\omega^2)^2 + (2\omega\nu)^2]^{1/2} \tag{C-12}$$

The result of solving equation (C-5) is:

$$\frac{A}{B} = - \frac{\omega_g^4}{2\omega_p^2} \cos\phi \tag{C-13}$$

The above quantities are substituted into Equations (C-3) and (C-7), the result being

$$\tan\phi = \frac{\omega\nu + \dfrac{\omega_g^4}{4r^2} 2\omega\nu}{\omega_p^2 - \omega^2 - \dfrac{\omega_g^4(\omega_p^2 - 4\omega^2)}{4r^2}} \tag{C-14}$$

$$B\cos\phi = \frac{-1}{\left[\omega_p^2 - \omega^2 - \dfrac{\omega_g^4(\omega_p^2 - 4\omega^2)}{4r^2}\right]\sec^2\phi - \dfrac{\omega_g^4}{2\omega_p^2}} \tag{C-15}$$

Finally substituting back into Equation (C-3) the average plasma acceleration is:

$$\left\langle \frac{d^2 Z_m}{dt^2} \right\rangle_{AV} = \frac{e}{2M} \omega_g^2 E_o \frac{\omega_p^2 - \omega^2 - \dfrac{\omega_g^4 (\omega_p^2 - 4\omega^2)}{4r^2}}{\left[\omega_p^2 - \omega^2 - \dfrac{\omega_g^4(\omega_p^2 - 4\omega^2)}{4r^2}\right] - \dfrac{\omega_g^4}{2\omega_p^2}\left[\omega_p^2 - \omega^2 - \dfrac{\omega_g^4(\omega_p^2 - 4\omega^2)}{4r^2}\right] + \left(\omega\nu + \dfrac{\omega_g^4\, 2\omega\nu}{4r^2}\right)^2} \quad \text{(C-16)}$$

where

$$r^2 = (\omega_p^2 - 4\omega^2)^2 + (2\omega\nu)^2 \quad \text{(C-17)}$$

If ω_g^4 is very small compared to r^2, the analysis is similar to the original theory, and Equation C-16 reduces to an equation similar to Equation 7. When the applied frequency is close to the critical frequency and the electron collision frequency is small, the limit of applicability of the original theory is

$$\frac{\partial E}{\partial Z} << 3 \frac{m}{e} \omega_p^2 \quad \text{(C-18)}$$

For an average field gradient of $dE/dz = KE$ where $K \cong 1.94\ cm^{-1}$ for the present apparatus, it is possible to calculate the theoretical final plasma velocity from Equation (C-16). One curve is shown in Figure 19 and is compared to the corresponding curve from the simple theory. For this particular case a deviation of 10% in the plasma velocity occurs when the field gradient is only 0.3 of $\omega_p^2\, m/e$. The analysis shows that the effects of large field gradients are important for the experiments. It does not help in explaining the differences between theory and experiment shown in Figure 16, since the improved theory tends to increase the discrepancy, rather than reduce it.

It should be noted that the application of this analysis has been made only for the region beyond the field maximum, i.e., the main accelerating region. It has been assumed that the transition between the zero field inside the plasma source and the

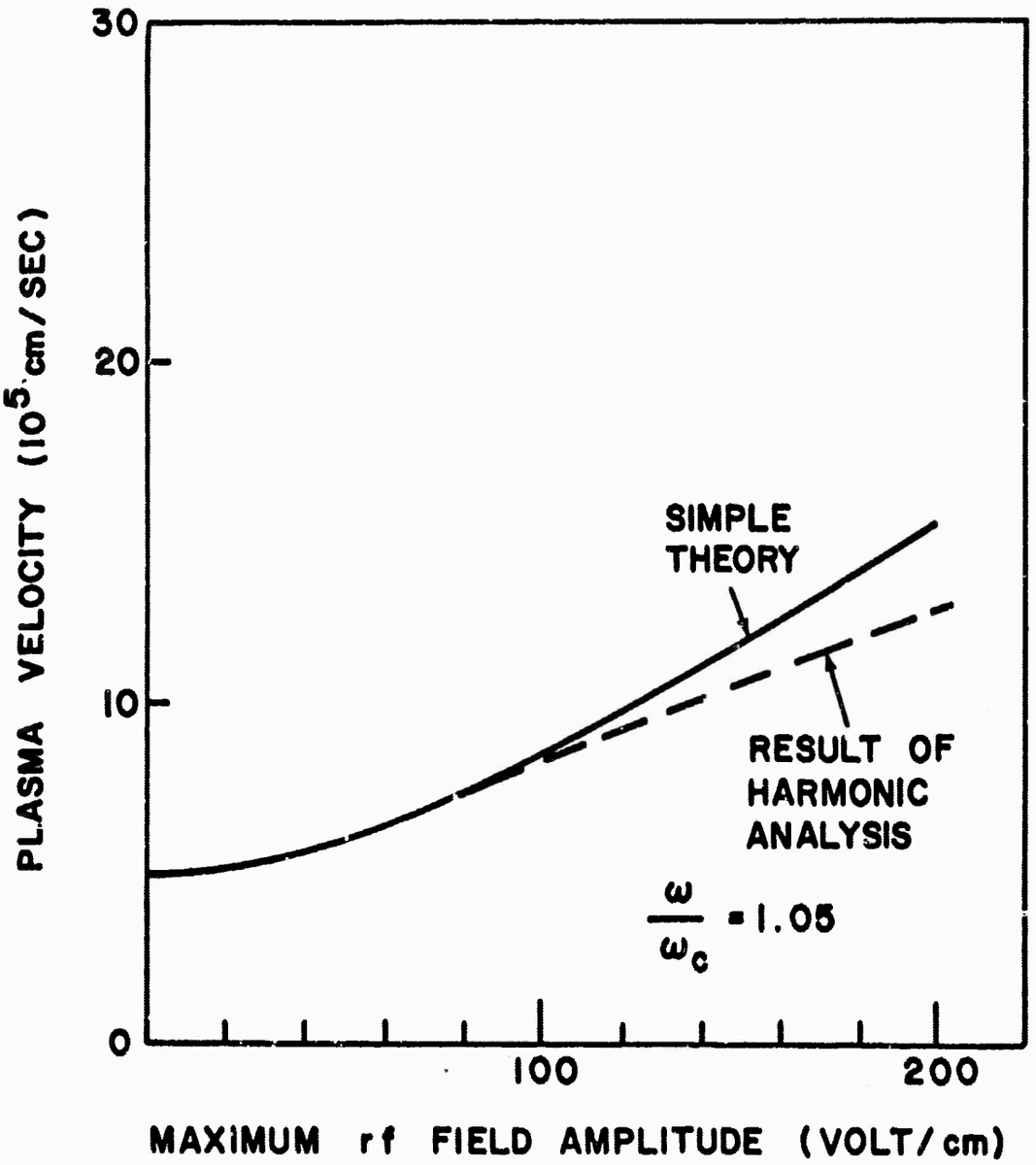

Figure 19. Effect of Large Field Gradients on Plasma Velocity

maximum field outside the orifice is so sharp that there are no acceleration effects. This is equivalent to assuming that the field gradients in this region are very large. The experiments discussed in Appendix E indicate that this assumption fails to hold for rf voltages below 100 volts. At these low voltages deceleration may take place before the plasma enters the maximum field region, and thus might decrease the final plasma velocities observed. Such an effect would increase the observed slope of plasma velocity vs. rf field, and might explain the slope discrepancy between the present theory and experiment which is shown in Figure 16.

APPENDIX D

ION TEMPERATURE DETERMINATION FROM AMBIPOLAR DIFFUSION

Plasma generated by the mercury igniter source moves into the rf interaction region by ambipolar diffusion. A measurement of the ambipolar diffusion velocity together with the plasma electron temperature will give a determination of the plasma ion temperature.

The plasma diffusion velocity, v , for a two-charge system is[19]

$$\bar{v} = \frac{v^+K^- + v^-K^+}{K^+ + K^-} \tag{D-1}$$

where (+) denotes ions and (-) denotes electrons, v is the diffusion velocity of particles in the absence of oppositely charged particles, and K is the mobility. Since the mobility of the ions is much less than that of the electrons, the diffusion velocity is approximately

$$\bar{v} = v_T^+ + v_T^- \frac{K^+}{K^-} \tag{D-2}$$

where v_T denotes thermal velocity.

By the Einstein relationship,[20]

$$\frac{K^+}{K^-} = \frac{D^+T^-}{D^-T^+} \tag{D-3}$$

where D is the diffusion constant of the particles and T is the temperature. The diffusion constant can be expressed in terms of the mean free path L and the

thermal velocity[21]

$$D = \left(\frac{1}{3}\right) L \ v_T \tag{D-4}$$

The mean free path for Hg ions in a Hg gas is

$$L^+ = \sqrt{2}\ L_g \tag{D-5}$$

and for 20,000°K electrons in a Hg gas[22]

$$L^- = 2.8\ L_g \tag{D-6}$$

where L_g is the mean free path of the neutral Hg atoms.

The ratio of the ion to the electron diffusion constant is

$$\frac{D^+}{D^-} = \frac{\sqrt{2}\ v_T^+}{2.8\ v_T^-} = .5\ \frac{v_T^+}{v_T^-} \tag{D-7}$$

Combining equations (2), (3) and (7)

$$\bar{v} = v_T^+ \left(1 + .5\ \frac{T^-}{T^+}\right) \tag{D-8}$$

The average thermal velocity of the ions is

$$v_T^+ = 4 \sqrt{\frac{kT^+}{2\pi M}} \tag{D-9}$$

where M is the mass of the ions k is the Boltzman constant.

The ambipolar diffusion velocity is therefore, a function of the electron and ion temperatures and the mass of the ions,

$$\bar{v} = \sqrt{\frac{5kT^+}{\pi M}} \left(1 + .5\ \frac{T^-}{T^+}\right) \tag{D-10}$$

Solving for T^+

$$T^+ = -.5T^- + \frac{\pi M \bar{v}}{16k}\left[\bar{v} - \sqrt{\bar{v}^2 - \frac{16kT^-}{\pi M}}\right] \qquad \text{(D-11)}$$

When $T^+ \ll T^-$

$$T^+ = \frac{2}{\pi}\,\frac{k}{M}\left(\frac{T^-}{\bar{v}}\right)^2 \qquad \text{(D-12)}$$

APPENDIX E

EFFECT OF RF VOLTAGE ON MAGNITUDE OF PROBE CURRENT

A. INTRODUCTION

Experiments on probe currents at low rf voltages yielded the following results. The peak current on a probe decreased (by a factor of ten) as the rf voltage was increased, and after reaching a minimum then increased with voltage. The experimental conditions are describe in section IV and the results are shown in Figure 15. These experimental results can be qualitatively explained as follows: As the rf voltage increases, the field barrier (proportional to the square of the maximum field) increases in the region outside the source orifice. The number of electrons that have sufficient thermal energy to cross the barrier decreases as the barrier is raised. For higher voltages, electrons of the proper phase can be accelerated all the way to the maximum field point in less than one rf cycle, and are not contained by the field barrier; hence, the number of electrons observed increases for higher rf voltages. Not only the decrease and increase of electrons with rf voltage, but also the magnitude of the rf voltage at which the minimum is observed, can be explained by the theory.

The decrease of intensity with increasing rf voltage and the later increase are due to different effect, and the observed sharp minimum is partly a coincidence. Under different circumstances the minimum might be quite broad, and the electrons might be contained by the field barrier for several orders of magnitude change in rf voltage. The theory is therefore divided in two parts, the first explaining the decrease, and the second the increase.

The theory is based on the behavior of the electrons, and neglects their interactions with the ions. A theory that includes the electron-ion interactions in the region in which the plasma enters the rf field has not yet been formulated, but there is reason to believe that for the data shown in Figure 15 these interactions are not important.

B. DECREASE IN INTENSITY

The deceleration of electrons for an applied frequency much greater than the plasma frequency, is given by theory[1] as

$$\frac{d^2\bar{Z}}{dt^2} = -\frac{e^2}{2m^2}\,\frac{E}{\omega^2}\,\frac{\partial E}{\partial Z} \qquad \text{(E-1)}$$

If an electron starts inside the igniter source with an initial velocity v_i in a region of no electric field, integration of equation E-1 shows that this velocity must be greater than a certain value, depending on the maximum electric field E_{max}, in order that the electrons pass the field maximum.

$$v_i > \frac{e}{\sqrt{2}\,m\omega}\,E_{max} \qquad \text{(E-2)}$$

It is assumed that the electron velocities have a Maxwell distribution, n_ξ, which for velocities in one specified direction is

$$n_\xi = \frac{n}{\sqrt{\pi}\,v_T}\,e^{-\frac{\xi^2}{v_T^2}} \qquad v_T^2 = \frac{2KT}{m} \qquad \text{(E-3)}$$

where T is the temperature of the electrons. The observed density of electrons will be proportional to the number of electrons with a velocity greater than the minimum, i.e.,

$$N = \int_{v_i}^{\infty} n_\xi\, d\xi = \frac{n}{\sqrt{\pi}} \int_{x}^{\infty} e^{-x^2}\, dx \qquad \text{(E-4)}$$

where

$$x = \frac{v_i}{v_T} = \frac{e E_{max}}{2 \omega \sqrt{m k T}} \qquad \text{(E-5)}$$

If the density of electrons N is plotted as a function of x, the result as shown in Figure 20 is the familiar integral of the error curve. If the slope at $x = 0$ is extrapolated to the x-axis, the intercept is a characteristic x_c, which is equal to

$$x_c = \frac{-(I)_o}{(dI/dx)_o} = \frac{n/2}{n/\sqrt{\pi}} = \frac{\sqrt{\pi}}{2} \qquad \text{(E-6)}$$

The curve for N vs. maximum electric field would have exactly the same shape, with the scale factor for the x-axis being given in Equation E-5. Solving for the characteristic electric field, the result is

$$E_c = \frac{\omega \sqrt{\pi m k T}}{e} \qquad \text{(E-7)}$$

where m and e are the mass and charge of the electron and k is the Boltzmann constant. In the present experiment the applied frequency was $\omega/2\pi = 140\ Mc$, and the measured electron temperature T was $20,000^{\circ}K$ as reported in section IV. The calculated characteristic field is then:

$$E_c = 47\ v/cm \qquad \text{(E-8)}$$

This field is equivalent to an rf potential of 55 volts in the present experiment. If the first part of the curve in Figure 15 is extrapolated, the x-axis intercept is about 60 volts, which is in agreement with the theory.

C. INCREASE IN INTENSITY

The theory of the electric field barrier assumes that the particle makes several oscillations which result in a net deceleration. If the amplitude of oscillation becomes of the same order of magnitude as the extent of the region of the gradient,

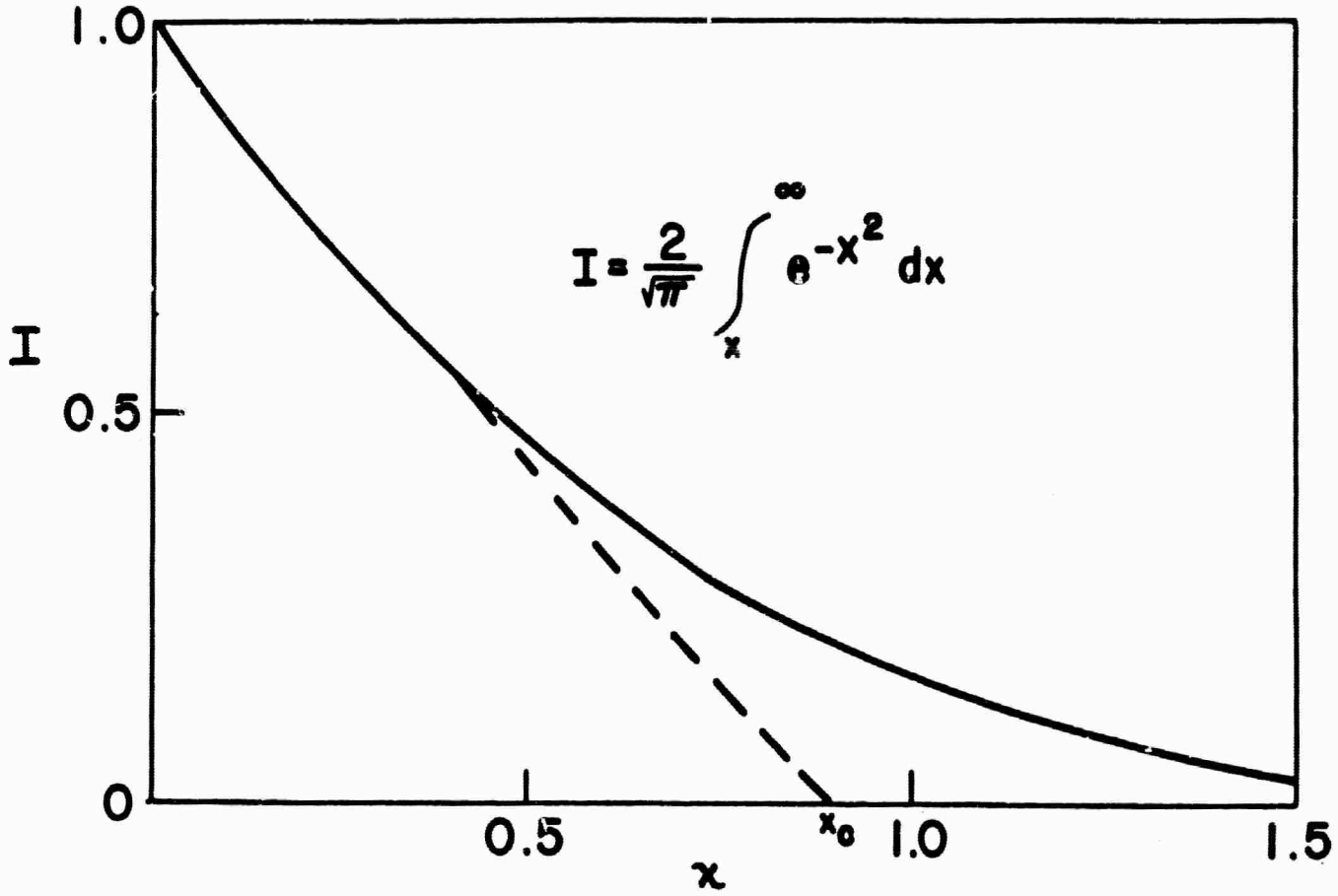

Figure 20. Probability Integral

electrons that arrive during a certain phase of the rf cycle will not be decelerated. The amplitude of the electron oscillations, if ion interactions are neglected, is

$$|\delta| = \frac{e}{m}\frac{E}{\omega^2} \qquad \omega \gg \omega_p \qquad \text{(E-9)}$$

The distance D, in which the electric field increases from a small value such as 1% to its maximum value outside the orifice, is 0.1 cm, as can be seen in Figure 5. Setting this distance equal to $|\delta|$ above, the equation can be solved for the electric field at which electrons will start to leak through the potential barrier.

$$E = \frac{D\,m\,\omega^2}{e} = 45\ v/cm \qquad \text{(E-10)}$$

This field at which electrons begin to leak through the rf barrier is equivalent to an rf potential of 55 volts. This is an excellent agreement with Figure 15; as the rf potential is increased beyond this limit, a larger number of electrons pass through the barrier.

D. CONCLUSIONS

Equation E-10 should be compared with Equation E-7.

Decrease:

$$E_c = \frac{\omega\sqrt{nmkT}}{e} = 47\ v/cm \qquad \text{(E-7)}$$

Increase:

$$E = \frac{Dm\omega^2}{e} = 45\ v/cm \qquad \text{(E-10)}$$

If any one of the factors in the equation is changed, the decrease and increase would no longer be at the same field, and the shape of the intensity vs. voltage curve would be quite different. If Equation E-10 had had a much smaller numerical result than Equation E-7 the probe current would not drop by a factor of five, and if it had been

higher. the minimum would be much broader. The minimum should indeed become broader if the orifice diameter or the applied frequency is increased, while it will be reduced in magnitude if the initial electron temperature is increased.

The theory can be compared with the experimental data shown in Figure 15. The theory is in good agreement as to the sharp minimum observed, and the value of the electric field at which this takes place. There is also reasonable agreement between the shape of the curve in Figure 20 and the decrease in intensity shown in Figure 15.

VII. LIST OF REFERENCES

1. Semi-Annual Report "Research on Plasma Acceleration by Electric Field Gradient" Contract No. AF49(638)-658, Astro-Electronic Products Division, Radio Corporation of America (Dec. 1959).

2. Second Symposium on Advance Propulsion Concepts, ARDC, (Boston, Oct. 1959).

3. G.M. Giannini, "The Arc Jet", Second Symposium on Advance Propulsion Concepts, ARDC, Boston, Oct. 1959.

4. W. Bostick, Phys. Rev. 106, 404 (1957).

5. A.C. Kolb, Phys. Rev. 107, 345 (1957).

6. M.L. Good, "A Proposed Particle Containment Device" Contract No. W-7405-eng-48 Radiation Laboratory, University of California UCRL 4146 (July 1953).

7. E.S. Weibel, "Confinement of a Plasma Column by Radiation Pressure", The Plasma in a Magnetic Field, ed. by R.K.M. Landshoff, (Stanford: Stanford University Press, 1958), 60-67.

8. H.A.H. Boot, S.A. Self, R.B.R. - Shersby-Harvie, J. Electronics and Control. 4, 434 (1958).

9. A.B. Gapanov, and M.A. Miller, J. Exptl. Theoret. Phys. (USSR) 34, 242 (1958), Soviet Phys. JETP 7, 168 (1958).

10. F.B. Knox, Australian Journal Phys. 10, 565 (1957).

11. J.V. Butler, A.J. Hatch, and A.J. Ulrich, "Proceedings of the Second United Nations International Conference on the Peaceful Uses of Atomic Energy" (United Nations, Geneva, 1958), Vol. 32, p.324.

12. A.A. Vedenov, V.M. Glagolev, et al; "Proceedings of the Second United Nations International Conference on the Peaceful Uses of Atomic Energy" (United Nations, Geneva, 1958), Vol. 32, p. 239.

13. A.B. Gapanov, and M.A. Miller, J. Exptl. Theoret. Phys. (USSR) 34, 751 (1958). Soviet Phys. - JETP 7, 515 (1958).

14. R.V. Hess, and K. Thom, "Plasma Acceleration by Guided Microwaves", Gas Dynamics Symposium, Northwestern University, Evanston, Ill. (Aug. 1959).

15. L. Tonks, Phys. Rev. 37, 1462 (1931).

16. J.D. Cobine, Gaseous Conductors, (Dover 1958) 134-142.

17. K.G. Hernqvist - Private Communication.

18. J.A. Stratton, Electromagnetic Theory (McGraw-Hill Book Company, Inc., New York 1941), p. 215.

19. J.D. Cobine, Gaseous Conductors, (Dover 1958) 48-53.

20. A. Einstein, Ann Physik 17, 549 (1905).

21. J.D. Cobine, Gaseous Conductors, (Dover 1958) 26-32.

22. R.B. Brode, Rev. Modern Phys. 5, 257 (1933).
H. Margenau and F.P Adler, Phys, Rev. 79, 970 (1950).
A.V. Engel and M. Steenbeck, Elektrische Gasentladungen, (Springer 1932) 39.